

Lepton-flavor universality violation in R_K and $R_{D^{(*)}}$ from warped space

Eugenio Megías^a, Mariano Quirós^b, Lindber Salas^b

^a*Departamento de Física Teórica, Universidad del País Vasco UPV/EHU,
Apartado 644, 48080 Bilbao, Spain*

^b*Institut de Física d'Altes Energies (IFAE),
The Barcelona Institute of Science and Technology (BIST),
Campus UAB, 08193 Bellaterra (Barcelona) Spain*

Abstract

Some anomalies in the processes $b \rightarrow s\ell\ell$ ($\ell = \mu, e$) and $b \rightarrow c\ell\bar{\nu}_\ell$ ($\ell = \tau, \mu, e$), in particular in the observables R_K and $R_{D^{(*)}}$, have been found by the BaBar, LHCb and Belle Collaborations, leading to a possible lepton flavor universality violation. If these anomalies were confirmed they would inevitably lead to physics beyond the Standard Model. In this paper we try to accommodate the present anomalies in an extra dimensional theory, solving the naturalness problem of the Standard Model by means of a warped metric with a strong conformality violation near the infra-red brane. The R_K anomaly can be accommodated provided that the left-handed bottom quark and muon lepton have some degree of compositeness in the dual theory. The theory is consistent with all electroweak and flavor observables, and with all direct searches of Kaluza-Klein electroweak gauge bosons and gluons. The fermion spectrum, and fermion mixing angles, can be reproduced by mostly elementary right-handed bottom quarks, and tau and muon leptons. Moreover the $R_{D^{(*)}}$ anomaly requires a strong degree of compositeness for the left-handed tau leptons, which turns out to be in tension with experimental data on the $g_{\tau_L}^Z$ coupling, possibly unless some degree of fine-tuning is introduced in the fixing of the CKM matrix.

Contents

1	Introduction	3
2	Lepton-flavor universality violation in R_K	8
3	Other $b \rightarrow s\ell^+\ell^-$ processes	12
4	Constraints	14
4.1	Radiative corrections to the Z -couplings	15
4.2	LHC Drell-Yan dilepton resonance searches	15
4.3	Direct Drell-Yan KK gluon searches	17
4.4	Dimuon resonance from bottom-bottom fusion	19
4.5	Flavor observables	20
5	The $b \rightarrow s\nu\bar{\nu}$ and $b \rightarrow s\tau\tau$ modes	23
6	Lepton-flavor universality violation in $R_{D^{(*)}}$	25
6.1	Ditau resonance from bottom-bottom fusion	28
6.2	Lepton flavor universality tests	29
6.3	The $Z\bar{\tau}\tau$ coupling	30
7	Conclusions and outlook	31

1 Introduction

While direct signals of new physics seem to be elusive up to now at the Large Hadron Collider (LHC), there exist anomalies showing up at the LHC, mainly by the LHCb Collaboration, as well as at electron collider B -factories, in particular by the BaBar and Belle Collaborations at SLAC and KEK, respectively. In the absence of direct experimental signatures of theories restoring the Standard Model naturalness, a legitimate attitude is to figure out which are the natural theories whose *direct detection should be hidden* from the actual experimental conditions, but that can accommodate possible explanations of (part of) the existing anomalies. This one is the point of view we will adopt in this paper.

There are two main ultra-violet (UV) completions of the Standard Model which can restore its naturalness and solve the Higgs hierarchy problem: **i)** Supersymmetry, where the Higgs mass is protected by a (super)symmetry; and, **ii)** Extra dimensional theories with a warped extra dimension, by which the Planck scale is warped down to the TeV scale along the extra dimension [1], or its dual, where the Higgs is composite and melts beyond the condensation scale at the TeV.

In this paper we will use the latter set of theories. In particular we will consider a set of warped theories with a strong deformation of conformality towards the infra-red (IR) brane [2–12], such that the Standard Model can propagate in the bulk of the fifth dimension, consistently with all measured electroweak observables. The theory is characterized by the superpotential

$$W(\phi) = 6k(1 + e^{a_0\phi})^{b_0} \tag{1.1}$$

where a_0 and b_0 are real (dimensionless) parameters which govern the back reaction on the gravitational metric $A(y)$, ϕ is the (dimensionless) scalar field stabilizing the fifth dimension and k is a parameter with mass dimension providing the curvature along the fifth dimension. We will not specify here the details of the five-dimensional (5D) model, as they were widely covered in the literature, Refs. [2–12], which we refer the reader to ¹. In this paper we will consider the superpotential of Eq. (1.1), with the particular values of the parameters

$$b_0 = 2, \quad a_0 = 0.15, \tag{1.2}$$

although somewhat similar results could equally well be obtained with different values. As we will see, these particular values minimize the impact of Kaluza-Klein (KK) modes in the electroweak observables and thus leave more room to accommodate possible anomalies.

¹For reviews see e.g. Refs. [9, 13].

In our model the Standard Model fermions $f_{L,R}$ propagate in the bulk of the extra dimension and their zero mode wave function, as determined by appropriate boundary conditions and the 5D Dirac mass $M_{f_{L,R}}(y) = \mp c_{f_{L,R}} W(\phi)$, depend on the real parameters $c_{L,R}$ which, in turn, determine the degree of compositeness of the corresponding field in the dual theory: composite (elementary) fermions are localized towards the IR (UV) brane and their corresponding parameter satisfies the relation $c_{f_{L,R}} < 0.5$ ($c_{f_{L,R}} > 0.5$). In particular their wave function is given by

$$f_{L,R}(y, x) = \frac{e^{(2-c_{L,R})A(y)}}{\left(\int dy e^{A(1-2c_{L,R})}\right)^{1/2}} f_{L,R}(x), \quad (1.3)$$

where $f_{L,R}(x)$ is the four-dimensional (4D) spinor.

Our choice of the 5D gravitational metric guarantees that the correction to the universal (oblique) observables, encoded in the Peskin-Takeuchi variables S, T, U [14], and the non-universal ones, in particular the shifts in the couplings $Z\bar{f}f$ where $f = b, \tau, \mu, e$, stay below their experimental values as we now show.

Oblique observables

In our model they are given by the following expressions [4]

$$\begin{aligned} \alpha_{EM}\Delta T &= s_W^2 \frac{m_Z^2}{\rho^2} k^2 y_1 \int_0^{y_1} [1 - \Omega_h(y)]^2 e^{2A(y)-2A(y_1)} dy, \\ \alpha_{EM}\Delta S &= 8c_W^2 s_W^2 \frac{m_Z^2}{\rho^2} k^2 y_1 \int_0^{y_1} \left(1 - \frac{y}{y_1}\right) [1 - \Omega_h(y)] e^{2A(y)-2A(y_1)} dy, \end{aligned} \quad (1.4)$$

and $\alpha_{EM}\Delta U \simeq 0$, where $\rho = ke^{-A(y_1)}$, $\Omega_h(y) = \frac{\omega(y)}{\omega(y_1)}$, and $\omega(y) = \int_0^y h^2(\bar{y}) e^{-2A(\bar{y})} d\bar{y}$, where the Higgs profile is taken to be $h(y) = h(0) \exp(\alpha y)$ with $\alpha = 2A(y_1)/ky_1$. The present experimental bounds on the S and T parameters are given by [15]

$$\Delta S = 0.07 \pm 0.08, \quad \Delta T = 0.10 \pm 0.07 \quad (\rho \simeq 0.90). \quad (1.5)$$

We show in Fig. 1 plots of ΔS and ΔT , as functions of a_0 , for fixed value of $m_{KK} = 2$ TeV, and $b_0 = 2$. We can see that the contribution to the S and T parameters implies the 2σ interval

$$0.1 \lesssim a_0 \lesssim 0.3. \quad (1.6)$$

In order to minimize the contribution to oblique parameters we will choose, from here on, the value $a_0 = 0.15$.

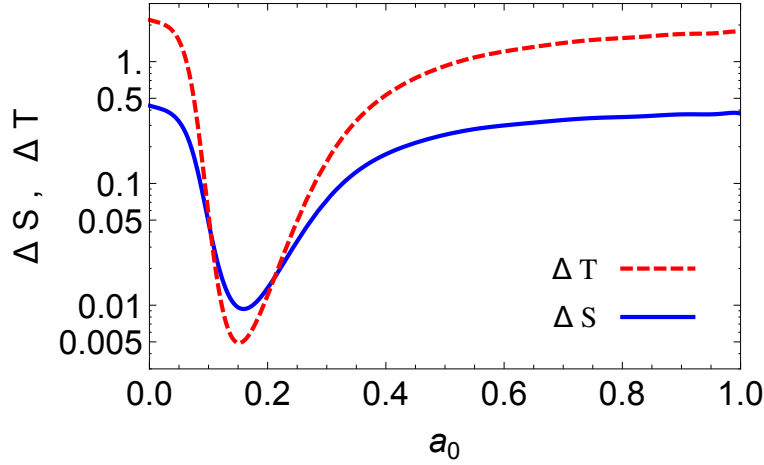


Figure 1: Contribution to the S and T parameters from the gauge KK modes as a function of a_0 . We have considered $b_0 = 2$ and $m_{KK} = 2$ TeV.

The $Z\bar{f}f$ coupling

The Z boson coupling to SM fermions $f_{L,R}$ with a sizeable degree of compositeness can be modified by two independent effects: one coming from the vector KK modes and the other from the fermion KK excitations. The distortion in the couplings can be straightforwardly written as a sum over the contributions of the various KK modes, as shown in Fig. 2, thus obtaining the full result [8, 16]

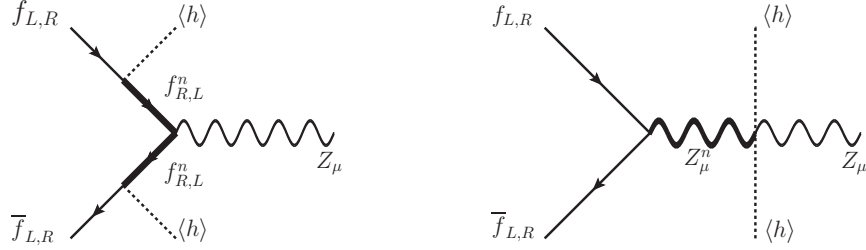


Figure 2: Diagrams contributing to $\delta g_{f_{L,R}}/g_{f_{L,R}}$.

$$\delta g_{f_{L,R}} = -g_{f_{L,R}}^{SM} m_Z^2 \hat{\alpha}_{f_{L,R}} \pm g \frac{v^2}{2} \hat{\beta}_{f_{L,R}}, \quad (1.7)$$

where $g_{f_{L,R}}^{SM}$ denotes the (tree-level) Z coupling to the $f_{L,R}$ fields in the SM, while

$$\begin{aligned}\hat{\alpha}_{f_{L,R}} &= y_1 \int_0^{y_1} e^{2A} \left(\Omega_h - \frac{y}{y_1} \right) (\Omega_{f_{L,R}} - 1) , \\ \hat{\beta}_{f_{L,R}} &= Y_f^2 \int_0^{y_1} e^{2A} \left(\frac{d\Omega_{f_{R,L}}}{dy} \right)^{-1} (\Gamma_f - \Omega_{f_{R,L}})^2 ,\end{aligned}\quad (1.8)$$

with Y_f the 4D Yukawa coupling and

$$\Omega_{f_{L,R}}(y) = \frac{\int_0^y e^{(1-2c_{f_{L,R}})A}}{\int_0^{y_1} e^{(1-2c_{f_{L,R}})A}}, \quad \Gamma_f(y) = \frac{\int_0^y h e^{-(c_{f_L}+c_{f_R})A}}{\int_0^{y_1} h e^{-(c_{f_L}+c_{f_R})A}}. \quad (1.9)$$

It is easy to recognize that the two terms in Eq. (1.7) correspond, respectively, to the effects of the massive vector and fermion KK modes.

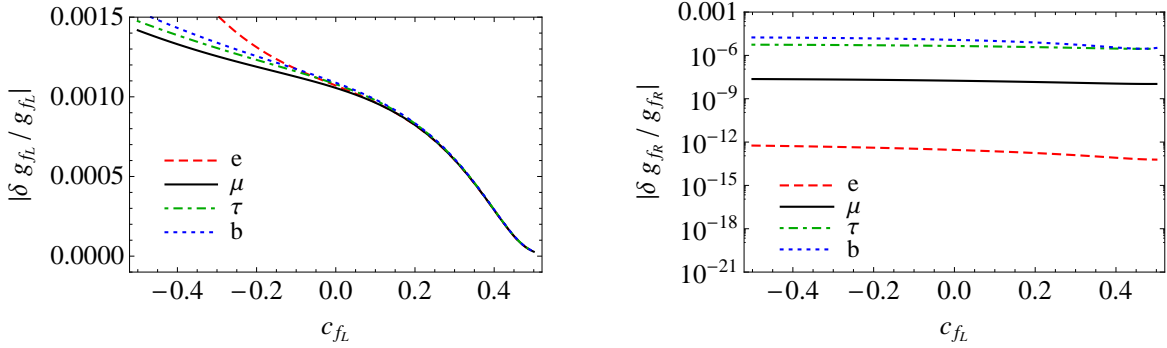


Figure 3: Contribution to $|\delta g_{f_L}/g_{f_L}|$ (left panel) and $|\delta g_{f_R}/g_{f_R}|$ (right panel) from KK modes for the electron (dashed red line), muon (solid black line), tau lepton (dot-dashed green line) and bottom quark (dotted blue line). The allowed region corresponds to the regime $|\delta g_{f_{L,R}}/g_{f_{L,R}}| \lesssim 10^{-3}$. We have considered $(c_{e_R}, c_{\mu_R}, c_{\tau_R}, c_{b_R}) = (0.85, 0.65, 0.55, 0.55)$.

We plot in Fig. 3 the value of $|\delta g_{f_L}/g_{f_L}|$ (left panel) and $|\delta g_{f_R}/g_{f_R}|$ (right panel) as a function of c_{f_L} for $f = e, \mu, \tau, b$ and $(c_{e_R}, c_{\mu_R}, c_{\tau_R}, c_{b_R}) = (0.85, 0.65, 0.55, 0.55)$. We can see that in all cases the constraint $|\delta g_{f_L}/g_{f_L}| \lesssim 10^{-3}$ [15] implies the mild constraint $c_{f_L} \gtrsim -0.5$. In particular from the values of $|\delta g_{\ell_{L,R}}/g_{\ell_{L,R}}|$ for $\ell = e, \mu, \tau$ we see that for $c_{\ell_L} \gtrsim -0.5$ no lepton flavor universality breaking appears at the Z -pole in agreement with the very strong LEP bounds on lepton non-universal couplings [15].

From Eq. (1.3) it is easily seen that the coupling of electroweak and strong KK gauge bosons to a fermion f with $c_f = 0.5$ vanishes due to the orthonormality of KK modes. Therefore if we assume that first generation quarks ($f = u, d$) are such that

$c_f \simeq 0.5$, it follows that Drell-Yan production of electroweak and strong KK gauge bosons from light quarks vanishes, or at least is greatly suppressed. Likewise the production of KK gluons by gluon fusion, or electroweak KK gauge bosons by vector-boson fusion, vanishes by orthonormality of KK modes, which can therefore only be produced by pairs, an energetically disfavored process. Therefore our theory satisfies our original strategy that *direct detection can be hidden*, depending on the degree of compositeness (or elementariness) of the Standard Model fermions.

On the experimental side, lepton flavor universality violation (LFUV) has been recently observed by the BaBar, Belle and LHCb Collaborations in the observables $R_{D^{(*)}}$ [17–23] and R_K [24]. In the present paper we will attempt to accommodate in our theory the actual experimental data exhibiting LFUV. The relevant involved fermions are b_L , τ_L and μ_L , characterized by the constants c_{b_L} , c_{τ_L} and c_{μ_L} . We will see that explaining all anomalies would require some degree of compositeness for the above fermions, a feature which is not motivated (as usually assumed for the Standard Model fermions) by the value of their masses, as it is e.g. the case of the top quark t_R . The required degree of compositeness of these not-so-heavy fermions has phenomenological consequences which, on the one hand, must be in agreement with all present and past experimental data, and on the other hand could trigger new phenomena to be searched for at present and future colliders.

Previous analyses in the literature have considered various *ad hoc* extensions of the Standard Model suitable to accommodate the anomalies, in particular including new gauge bosons [25–35], leptoquarks [36–50] and general effective field theory frameworks [51–55]². Anomalies in R_K , and $b \rightarrow s \ell \ell$ processes, have also been addressed in Randall-Sundrum [56–58] and flat space [59] extra dimensional scenarios. On the other hand, our approach is based on a *lepton flavor conserving* minimal model solving the naturalness problem of the Standard Model *without invoking any extra physics*.

The contents of this paper are as follows. The analysis of the R_K anomaly, as well as some comments about R_{K^*} , is performed in Sec. 2. As the result depends on the unitary transformations diagonalizing the quark mass matrices, and in the absence of a particular UV theory predicting the 5D Yukawa matrices, we will consider for the diagonalizing matrices $V_{u_{L,R}}$ and $V_{d_{L,R}}$ generic Wolfenstein-like parametrizations satisfying the relation $V_{u_L}^\dagger V_{d_L} = V_{\text{CKM}}$. Without making a statistical analysis of the parameter space we will assign generic values to the parameters which optimize the results. In Sec. 3 we impose constraints on the (almost) elementary electrons from the branching fraction of $\bar{B} \rightarrow \bar{K} e e$, as compared to its Standard Model value, and we

²In particular in Ref. [55] the effects of lepton flavor violation, as well as the renormalization group running, on lepton flavor universality violation have been explored.

adjust other observables, as e.g. $B_s \rightarrow \mu^+ \mu^-$, which appear in the $b \rightarrow s \mu^+ \mu^-$ decay process. We present in Sec. 4 the result of imposing the different constraints, including electroweak observables, direct searches and flavor constraints. All together they restrict the available region of parameters where the anomalies can be accommodated. An overproduction, with respect to the Standard Model prediction, in the branching ratios $\mathcal{B}(\bar{B} \rightarrow \bar{K} \tau \tau)$ and $\mathcal{B}(\bar{B} \rightarrow \bar{K} \nu \bar{\nu})$ can generically appear. This issue, as well as the region allowed by present data, is analyzed in Sec. 5. In Sec. 6 we consider the $R_{D^{(*)}}$ anomaly and we contrast it with the non-observation of flavor universality violation effects in the μ/e sector and with lepton flavor universality tests in tau decays. We will prove that the $R_{D^{(*)}}$ anomaly, along with a strict Wolfenstein-like parametrization of diagonalizing unitary matrices, is in tension with electroweak observables, in particular with experimental data on the coupling $g_{\tau L}^Z$. As we will point out this problem can be resolved by somehow slightly giving up on the Wolfenstein-like structure of diagonalizing matrices and thus allowing a small amount of fine-tuning when fixing the CKM matrix. Finally our conclusions and outlook are presented in Sec. 7.

2 Lepton-flavor universality violation in R_K

The LHCb Collaboration has determined the ratio of branching ratios $\mathcal{B}(\bar{B} \rightarrow \bar{K} \ell \ell)$ for muons over electrons yielding the result [24]

$$R_K \equiv R_K^{\mu/e} = \frac{\mathcal{B}(\bar{B} \rightarrow \bar{K} \mu \mu)}{\mathcal{B}(\bar{B} \rightarrow \bar{K} e e)} = 0.745_{-0.074}^{+0.090} \pm 0.036 \quad (2.1)$$

which, by combining systematic and statistical uncertainties in quadrature, implies a deviation $\sim 2.6\sigma$ with respect to the Standard Model prediction $R_K^{\text{SM}} = 1.0003 \pm 0.0001$ [60, 61].

One can interpret this result by using an effective description given by the $\Delta F = 1$ Lagrangian

$$\mathcal{L}_{eff} = \frac{4G_F}{\sqrt{2}} \frac{\alpha}{4\pi} V_{ts}^* V_{tb} \sum_i C_i \mathcal{O}_i, \quad (2.2)$$

where the Wilson coefficients $C_i = C_i^{\text{SM}} + \Delta C_i$, are the sum of a SM contribution C_i^{SM} and a new-physics one ΔC_i . The sum in Eq. (2.2) includes the operators

$$\begin{aligned} \mathcal{O}_9^\ell &= (\bar{s}_L \gamma_\mu b_L)(\bar{\ell} \gamma^\mu \ell), & \mathcal{O}_{10}^\ell &= (\bar{s}_L \gamma_\mu b_L)(\bar{\ell} \gamma^\mu \gamma_5 \ell), \\ \mathcal{O}_9^\ell &= (\bar{s}_R \gamma_\mu b_R)(\bar{\ell} \gamma^\mu \ell), & \mathcal{O}_{10}^\ell &= (\bar{s}_R \gamma_\mu b_R)(\bar{\ell} \gamma^\mu \gamma_5 \ell). \end{aligned} \quad (2.3)$$

for $\ell = \mu, e$.

After electroweak symmetry breaking the mass matrices for u and d -type quarks are diagonalized by the unitary matrices $V_{u_{L,R}}$ and $V_{d_{L,R}}$, and so their matrix elements, unlike those of the CKM matrix, are not measured experimentally and moreover are model dependent. In the absence of a general (UV) theory, providing the 5D Yukawa couplings $\hat{Y}_{u,d}$, we will just consider the general form for these matrices by assuming they reproduce the physical CKM matrix V , i.e. they satisfy the condition $V \equiv V_{u_L}^\dagger V_{d_L}$.

Given the hierarchical structure of the quark mass spectrum and mixing angles, we will then assume for the matrices V_{d_L} and V_{u_L} Wolfenstein-like parametrizations as

$$V_{d_L} = \begin{pmatrix} 1 - \frac{1}{2}\lambda_0^2 & \lambda_0 & A\lambda^2\lambda_0(1-r)(\rho_0 - i\eta_0) \\ -\lambda_0 & 1 - \frac{1}{2}\lambda_0^2 & A\lambda^2(1-r) \\ A\lambda^2\lambda_0(1-r)(1-\rho_0 - i\eta_0) & -A\lambda^2(1-r) & 1 \end{pmatrix}, \quad (2.4)$$

with values of the parameters $(r, \lambda_0, \rho_0, \eta_0)$ consistent with the hierarchical structure of the matrix, and

$$V_{u_L} = \begin{pmatrix} 1 - \frac{1}{2}(\lambda - \lambda_0)^2 & (\lambda_0 - \lambda)(1 + \frac{1}{2}\lambda_0\lambda) & (V_{u_L})_{13} \\ -(\lambda_0 - \lambda)(1 + \frac{1}{2}\lambda_0\lambda) & 1 - \frac{1}{2}(\lambda - \lambda_0)^2 & -A\lambda^2 r \\ (V_{u_L})_{31} & A\lambda^2 r & 1 \end{pmatrix}, \quad (2.5)$$

where

$$(V_{u_L})_{31} = A\lambda^3(\rho + i\eta) + A\lambda^2(1-r)[\lambda_0(1-\rho_0 - i\eta_0) - \lambda] \quad (2.6)$$

$$(V_{u_L})_{13} = A\lambda^3(1-\rho + i\eta) + A\lambda^2\lambda_0[(1-r)(\rho_0 - i\eta_0) - 1], \quad (2.7)$$

and where [15]

$$\lambda = 0.225, \quad A = 0.811, \quad \rho = 0.124, \quad \eta = 0.356 \quad (2.8)$$

are the parameters of the CKM matrix V in the Wolfenstein parametrization

$$V = \begin{pmatrix} 1 - \frac{1}{2}\lambda^2 & \lambda & A\lambda^3(\rho - i\eta) \\ -\lambda & 1 - \frac{1}{2}\lambda^2 & A\lambda^2 \\ A\lambda^3(1-\rho - i\eta) & -A\lambda^2 & 1 \end{pmatrix}. \quad (2.9)$$

The matrix forms of (2.4) and (2.5) guarantee the precise determination of the CKM matrix elements in (2.9). In particular, in numerical calculations, we will make the particular choice

$$\lambda_0 \simeq \mathcal{O}(\lambda), \quad \eta_0 \simeq \mathcal{O}(\eta), \quad 0 \lesssim r \lesssim 1, \quad 0 \lesssim \rho_0 \lesssim 1 \quad (2.10)$$

which guarantees the Wolfenstein-like structure of the matrices V_{d_L} and V_{u_L} .

Our theory contains the neutral current interaction Lagrangian

$$\mathcal{L} = \frac{g}{c_W} \sum_{X=Z,\gamma} \sum_n X_n^\mu (g_{f_L}^{X_n} \bar{f}_L \gamma_\mu f_L + g_{f_R}^{X_n} \bar{f}_R \gamma_\mu f_R) , \quad (2.11)$$

where $g_{f_{L,R}}^{X_n} = g_{f_{L,R}}^X G_{f_{L,R}}^n$ with

$$\begin{aligned} g_{f_L}^Z &= (T_{3f} - Q_f s_W^2), \quad g_{f_R}^Z = -Q_f s_W^2, \\ g_{f_L}^\gamma &= Q_f s_W c_W, \quad g_{f_R}^\gamma = Q_f s_W c_W \end{aligned} \quad (2.12)$$

and the couplings G_f^n defined as

$$G_f^n = \frac{\sqrt{y_1} \int e^{-3A} f_A^n(y) f^2(y)}{\sqrt{\int [f_A^n(y)]^2 \int e^{-3A} f^2(y)}}, \quad (2.13)$$

where $f_A^n(y)$ is the profile of the gauge boson n -KK mode and $f(y)$ the profile of the corresponding fermion zero-mode, as given by Eq. (1.3). The plot of $G_f^n(c)$ (for $n = 1$) as a function of the parameter c , which determines the localization of the fermion zero mode, is shown in Fig. 4. Notice that it vanishes for $c = 0.5$, as anticipated in Sec. 1, while it grows in the IR, and stabilizes itself around -0.1 in the UV.

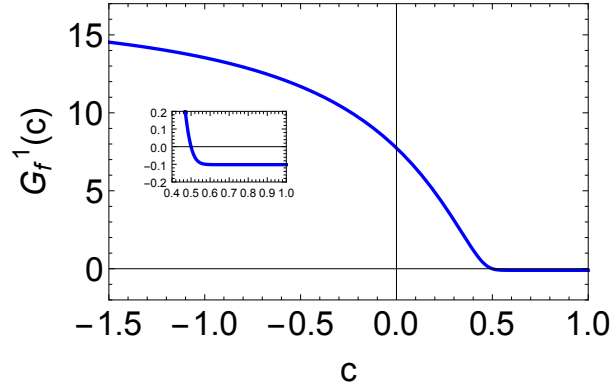


Figure 4: Coupling (normalized with respect to the 4D coupling) of a fermion zero-mode with the $n = 1$ KK gauge field, $W_\mu^{(n)}$, as a function of the fermion localization parameter c [cf. Eq. (2.13)].

In the following we will assume that the first and second generation quarks respect the universality condition. This implies an approximate accidental $U(2)_{q_L} \otimes U(2)_{u_R} \otimes U(2)_{d_R}$ global flavor symmetry, which is only broken by the Yukawa couplings [16]. For

simplicity in our numerical analysis we will moreover choose $c_{q_L^1} = c_{q_L^2} \equiv c_{q_L}$, as well as $c_{u_R} = c_{c_R} = c_{d_R} = c_{s_R} \equiv c_{q_R}$. The values $r = 0.75$ and $m_{KK} = 2$ TeV have been chosen, and will be adopted, without explicit mention, in the rest of the paper.

In our model, contact interactions can be obtained by the exchange of KK modes of the Z (Z_n) and the photon (γ_n). They give rise to the Wilson coefficients ³ [16]

$$\begin{aligned}\Delta C_9^{(\ell)\ell} &= -(1-r) \sum_{X=Z,\gamma} \sum_n \frac{2\pi g^2 g_{\ell_V}^{X_n} (g_{b_{L(R)}}^{X_n} - g_{q_{L(R)}}^{X_n})}{\sqrt{2} G_F \alpha c_W^2 M_n^2}, \\ \Delta C_{10}^{(\ell)\ell} &= (1-r) \sum_{X=Z,\gamma} \sum_n \frac{2\pi g^2 g_{\ell_A}^{X_n} (g_{b_{L(R)}}^{X_n} - g_{q_{L(R)}}^{X_n})}{\sqrt{2} G_F \alpha c_W^2 M_n^2}.\end{aligned}\tag{2.14}$$

where $g_{f_{V,A}}^{X_n} = g_{f_L}^{X_n} \pm g_{f_R}^{X_n}$. Using now the Standard Model prediction $C_9^{\text{SM}} = -C_{10}^{\text{SM}} \simeq 4.2$

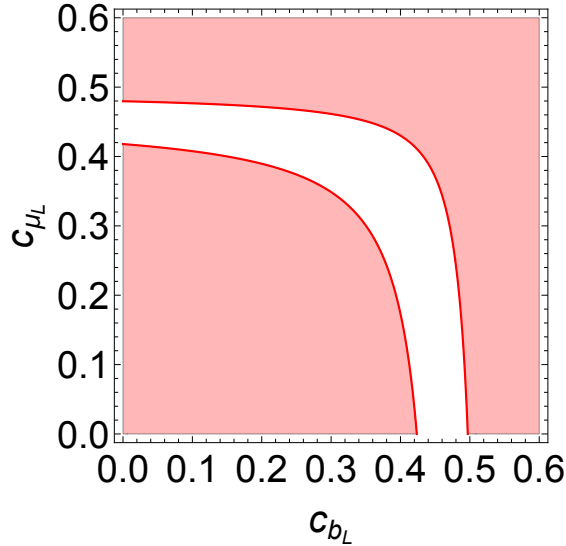


Figure 5: Region in the (c_{b_L}, c_{μ_L}) plane that accommodates the 2σ region $R_K \in [0.580, 0.939]$. We display the result for $c_{e_L} = 0.5$.

at the m_b scale, and following Ref. [62], we find the 2σ interval $0.580 < R_K < 0.939$, where we have combined statistical and systematic uncertainties in quadrature, while the observable R_K , in terms of the Wilson coefficients, is given by [38, 62]

$$R_K = \frac{|C_9^{\text{SM}} + \Delta C_9^\mu + \Delta C_9^{\prime\mu}|^2 + |C_{10}^{\text{SM}} + \Delta C_{10}^\mu + \Delta C_{10}^{\prime\mu}|^2}{|C_9^{\text{SM}} + \Delta C_9^e + \Delta C_9^{\prime e}|^2 + |C_{10}^{\text{SM}} + \Delta C_{10}^e + \Delta C_{10}^{\prime e}|^2}.\tag{2.15}$$

³Notice that the Wilson coefficients in Eq. (2.14) differ by a factor $(1-r)$ with respect to those in Ref. [16], where moreover we were assuming $V_{u_L} \simeq 1_3$ and $V_{d_L} = V$.

In Fig. 5 we show in the (c_{b_L}, c_{μ_L}) plane the 2σ region allowed by the experimental data on R_K , the region between the solid red lines, where we use the values $c_{e_L} = 0.5$, $c_{q_L} = c_{q_R} = 0.8$, $c_{b_R} = 0.55$ and $c_{\mu_R} = 0.65$. As we can see from this plot, both fermions b_L and μ_L must be localized towards the IR, and thus have to exhibit some degree of compositeness in the dual theory. Here we obtain the mild constraints

$$c_{b_L} \lesssim 0.50 \quad \text{and} \quad c_{\mu_L} \lesssim 0.49.$$

In fact as we can see from the plot of Fig. 5 the degrees of compositeness of b_L and μ_L are inversely proportional to each other.

To conclude this section, we would like to mention that the model prediction for the related observable R_{K^*} recently measured by the LHCb Collaboration [63] is $R_{K^*} \simeq R_K$. In fact a measurement of R_{K^*} in agreement with the Standard Model prediction $R_{K^*}^{\text{SM}} \simeq 1$ [61] would be in tension with our explanation of the R_K anomaly.

3 Other $b \rightarrow s\ell^+\ell^-$ processes

The values of $c_{e_{L,R}}$ are constrained by the LHCb measurement [24] of the branching ratio $\mathcal{B}(\bar{B} \rightarrow \bar{K}ee)$ and the 2σ result [38]

$$0.41 \lesssim R_K^e \equiv \frac{\mathcal{B}(\bar{B} \rightarrow \bar{K}ee)}{\mathcal{B}(\bar{B} \rightarrow \bar{K}ee)_{\text{SM}}} \lesssim 1.25 \quad (3.1)$$

where

$$R_K^e = \frac{|C_9^{\text{SM}} + \Delta C_9^e + \Delta C_9^{\prime e}|^2 + |C_{10}^{\text{SM}} + \Delta C_{10}^e + \Delta C_{10}^{\prime e}|^2}{2|C_9^{\text{SM}}|^2}. \quad (3.2)$$

The corresponding allowed region in the plane (c_{b_L}, c_{e_L}) is shown in the left panel of Fig. 6, where we use the values $c_{q_L} = c_{q_R} = 0.8$ and $c_{b_R} = 0.55$. We can see from the plot that values of c_{e_L} around $c_{e_L} = 0.5$ allow any value of c_{b_L} , as in particular for such value of c_{e_L} we have that $\Delta C_9^e = \Delta C_{10}^e$ and $\Delta C_9^{\prime e} = \Delta C_{10}^{\prime e}$, and the ratio (3.2) is one to linear order in the Wilson coefficients. Moreover for $c_{e_{L,R}} = 0.5$ the coupling of electrons to the KK modes of gauge bosons vanishes and there is no contribution to observables involving the electron. On the other hand this is not the case for muons, which accomplishes in our model the mechanism of lepton flavor universality violation from the new physics mediated by the KK modes of electroweak gauge bosons.

The rare flavor-changing neutral current decay $B_s \rightarrow \mu^+\mu^-$ has been recently observed by the LHCb Collaboration with a branching fraction [64]

$$\mathcal{B}(B_s \rightarrow \mu^+\mu^-) = (2.8_{-0.6}^{+0.7}) \times 10^{-9}, \quad (3.3)$$

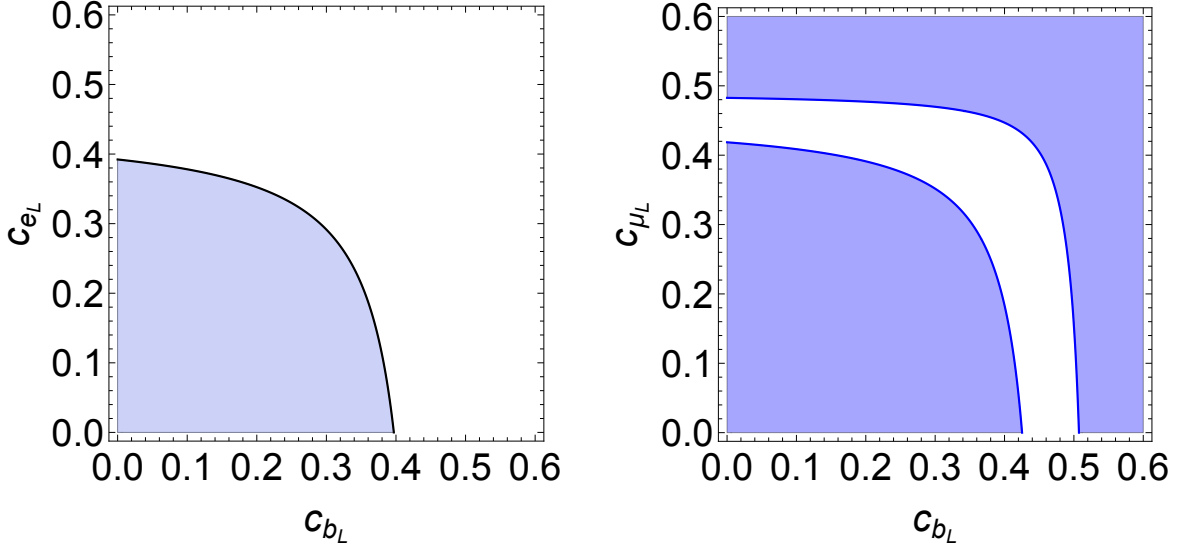


Figure 6: Left panel: Region in the plane (c_{b_L}, c_{e_L}) that accommodates the constraint on $\mathcal{B}(\bar{B} \rightarrow \bar{K}ee)$ given by Eq. (3.1). Right panel: Region in the plane (c_{b_L}, c_{μ_L}) that accommodates the 1σ region $R_0 \in [0.594, 0.962]$.

pretty consistent with the Standard Model prediction [65]

$$\mathcal{B}(B_s \rightarrow \mu^+ \mu^-)_{\text{SM}} = (3.66 \pm 0.23) \times 10^{-9}. \quad (3.4)$$

By combining the experimental and theoretical uncertainties in quadrature we can write the ratio

$$R_0 = \frac{\mathcal{B}(B_s \rightarrow \mu^+ \mu^-)}{\mathcal{B}(B_s \rightarrow \mu^+ \mu^-)_{\text{SM}}} = 0.765^{+0.197}_{-0.171} \quad (3.5)$$

while, in terms of the effective operator Wilson coefficients in Eq. (2.14), we have [49]

$$R_0 = \left| \frac{C_{10}^{\text{SM}} + \Delta C_{10}^{\mu} - \Delta C_{10}^{\prime\mu}}{C_{10}^{\text{SM}}} \right|^2. \quad (3.6)$$

The 1σ region allowed by R_0 is shown in the right panel plot of Fig. 6.

Global fits to the Wilson coefficients $\Delta C_{9,10}^{(\prime)\mu}$ have also been performed in the literature using a set of observables, including the branching ratios for $B \rightarrow K^* \ell \ell$, $B_s \rightarrow \phi \mu \mu$ and $B_s \rightarrow \mu \mu$, in Refs. [66–69]. However, as observed in Refs. [66, 67], removing the data on R_K from the fits, lepton universality can be restored at a slightly larger deviation than 1σ . As in our model we have the approximate relation $\Delta C_9 \simeq -\Delta C_{10}$, using the recent multi-observable fit (which includes $R_{K^{(*)}}$) from Ref. [70] we get the 2σ interval $\Delta C_9 \in [-0.93, -0.31]$. We shown in the plot of Fig. 7 the region in the (c_{b_L}, c_{μ_L}) plane that accommodates the previous constraint on C_9 , where we also superimpose

the plot from R_K in Fig. 5. As we can see the plot on the fitted value of C_9 slightly deviates from the plot in Fig. 5 on the experimental value of R_K . We can conclude that at present R_K is the main driving force for lepton flavor non-universality in the μ/e sector. For that reason, as our paper deals mainly with NP effects on lepton flavor non-universality, we will just consider in our analysis R_K data.

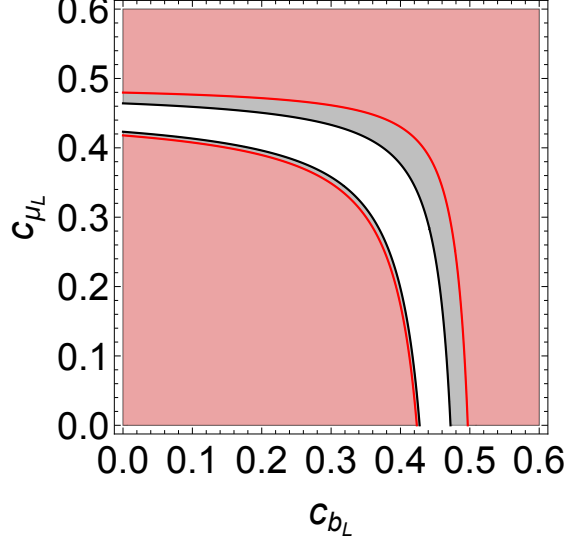


Figure 7: Region in the (c_{b_L}, c_{μ_L}) plane that accommodates the 2σ region $\Delta C_9 \in [-0.93, -0.31]$ from the fit of Ref. [70] (blank region inside gray bands). We overlap as well the allowed region coming from the R_K anomaly (blank region inside red bands).

4 Constraints

As we have seen in the previous sections lepton flavor non-universality, mainly in the observable R_K , imply different degree of compositeness mainly for the fermions b_L and μ_L , all of them localized towards the IR brane. This fact triggers modifications in the couplings of fermions with the Z gauge boson, which are very constrained by experimental data. In particular, the KK modes of electroweak gauge bosons can trigger, through the mixing with electroweak gauge bosons after electroweak symmetry breaking, a modification of the universal (oblique) observables which were already considered in Sec. 1. Moreover KK modes of the gluon can trigger $\Delta F = 2$ flavor violating effective operators, which are also very constrained by the experimental data. Finally, direct searches of electroweak gauge boson KK modes decaying into muons and taus, and direct searches of gluon KK modes decaying into top quarks, by Drell-Yan processes, do depend on the couplings of fermions to KK modes, which in turn depend on the

constants c_{b_L} , c_{τ_L} and c_{μ_L} , as we have seen in Fig. 4. All these constraints will be considered in this section.

4.1 Radiative corrections to the Z -couplings

Our fundamental theory contains the interaction Lagrangian of Eq. (2.11). Upon integration of the KK modes Z_n and γ_n we obtain the effective Lagrangian

$$\mathcal{L}_{eff} = \frac{C_n^{t\ell}}{M_n^2} (\bar{t}_L \gamma_\mu t) (\ell_L \gamma^\mu \ell_L) \quad (4.1)$$

where ⁴

$$C_n^{t\ell} = -\frac{g^2}{c_W^2} (g_{u_L}^Z g_{\ell_L}^Z + g_{u_L}^\gamma g_{\ell_L}^\gamma) G_{b_L}^n G_{\ell_L}^n. \quad (4.2)$$

Using the formalism of Ref. [55] the RG evolution of the operator $(\bar{t}_L \gamma_\mu t) (\bar{\ell}_L \gamma_\mu \ell_L)$ gives rise to the operator $(H^\dagger D_\mu H) (\bar{\ell}_L \gamma^\mu \ell_L)$, which in turn generates the shift $g_{\ell_L}^Z \rightarrow g_{\ell_L}^Z + \Delta g_{\ell_L}^Z$ with ⁵

$$\Delta g_{\ell_L}^Z = \frac{v^2}{M_n^2} \frac{1}{16\pi^2} \left[3y_t^2 C_n^{t\ell} \log \frac{M_n}{m_t} - \frac{g^4}{4} \left(1 - \frac{s_W^4}{9c_W^4} \right) G_{b_L}^n G_{\ell_L}^n \log \frac{M_n}{m_Z} \right]. \quad (4.3)$$

We can now use the fit from experimental data in Ref. [71]

$$g_{\mu_L}^Z = -0.2689 \pm 0.0011 \quad (4.4)$$

leading to the result ⁶

$$\Delta g_{\mu_L}^Z + \delta g_{\mu_L}^Z = (0.49 \pm 1.1) \times 10^{-3} \quad (4.5)$$

where $\delta g_{\mu_L}^Z$ stands for the tree-level contribution from the Z and fermion KK-modes in Eq. (1.7). The resulting 2σ allowed (white) region is shown in the plot of Fig. 8 in the (c_{b_L}, c_{μ_L}) plane. We can see that the permitted region is not in conflict with the plot of Fig. 5, where the allowed region consistent with the data on R_K was exhibited.

4.2 LHC Drell-Yan dilepton resonance searches

An additional experimental constraint comes from direct searches for high-mass resonances decaying into dilepton final states. The resonances Z_μ^n and γ_μ^n can be produced by Drell-Yan processes and decay into a pair of leptons as in Fig 9.

⁴In the language of Ref. [55] we have

$$C_3^{t_L \ell_L} = -\frac{g^2}{4} G_{b_L}^n G_{\ell_L}^n, \quad C_1^{t_L \ell_L} = \frac{g^2 s_W^2}{12 c_W^2} G_{b_L}^n G_{\ell_L}^n.$$

⁵We are neglecting here the contribution from Yukawa couplings other than the top quark.

⁶The recent fit from Ref. [72] yields $\Delta g_{\mu_L}^Z + \delta g_{\mu_L}^Z = (0.1 \pm 1.2) \times 10^{-3}$ fully consistent with Eq. (4.5).

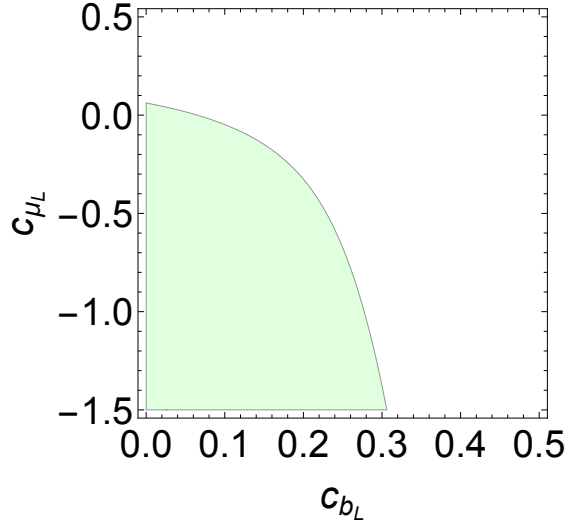


Figure 8: Region in the plane (c_{b_L}, c_{μ_L}) that accommodates $\Delta g_{\mu_L}^Z + \delta g_{\mu_L}^Z$ as shown in Eq. (4.5).

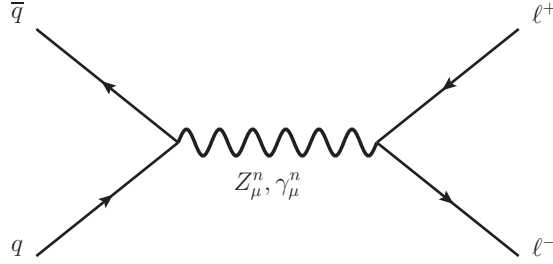


Figure 9: Diagrams contributing to the process $\sigma(pp \rightarrow Z_n/\gamma_n \rightarrow \ell^+\ell^-)$.

In the narrow width approximation the cross-section for the process $pp \rightarrow Z^n/\gamma^n \rightarrow \ell^+\ell^-$ approximately scales as

$$\sigma(pp \rightarrow Z_n/\gamma_n \rightarrow \ell^+\ell^-) \propto A_\ell = \sum_{X=Z,\gamma} A_\ell^{X^n},$$

$$A_\ell^{X^n} = \frac{(g_{\ell_L}^2 + g_{\ell_R}^2)(2g_{u_L}^2 + 2g_{u_R}^2 + g_{d_L}^2 + g_{d_R}^2)}{\sum_f (g_{f_L}^2 + g_{f_R}^2)}, \quad (4.6)$$

where all couplings refer to the $g_{f_{L,R}}^{X^n}$ couplings, and for simplicity we have omitted the superscript X^n . In the denominator the sum over f covers the three generation of quarks and leptons in the Standard Model. As this process is flavor conserving we are neglecting here the small correction from mixing angles.

The best bounds on dimuon resonances have been given by the ATLAS Collaboration [73] based on 3.2 fb^{-1} data at $\sqrt{s} = 13 \text{ TeV}$. ATLAS obtained a 95% CL bound on

the sequential Standard Model (SSM) Z'_{SSM} gauge boson mass as $M_{Z'_{SSM}} \gtrsim 3.36$ TeV. After rescaling the bound we get for our 2 TeV KK-mode the bound $A_\mu \lesssim 0.003$. The allowed region in the plane (c_{q_L}, c_{μ_L}) is shown in the left panel of Fig. 10. Similarly the strongest bounds on ditau resonances have been obtained by the CMS Collaboration [74] based on 2.2 fb^{-1} data at $\sqrt{s} = 13$ TeV. CMS got the 95% CL bound $M_{Z'_{SSM}} \gtrsim 2.1$ TeV. After rescaling this result it translates into $A_\tau \lesssim 0.022$. The allowed region in the plane (c_{q_L}, c_{τ_L}) is shown in the right panel of Fig. 10.

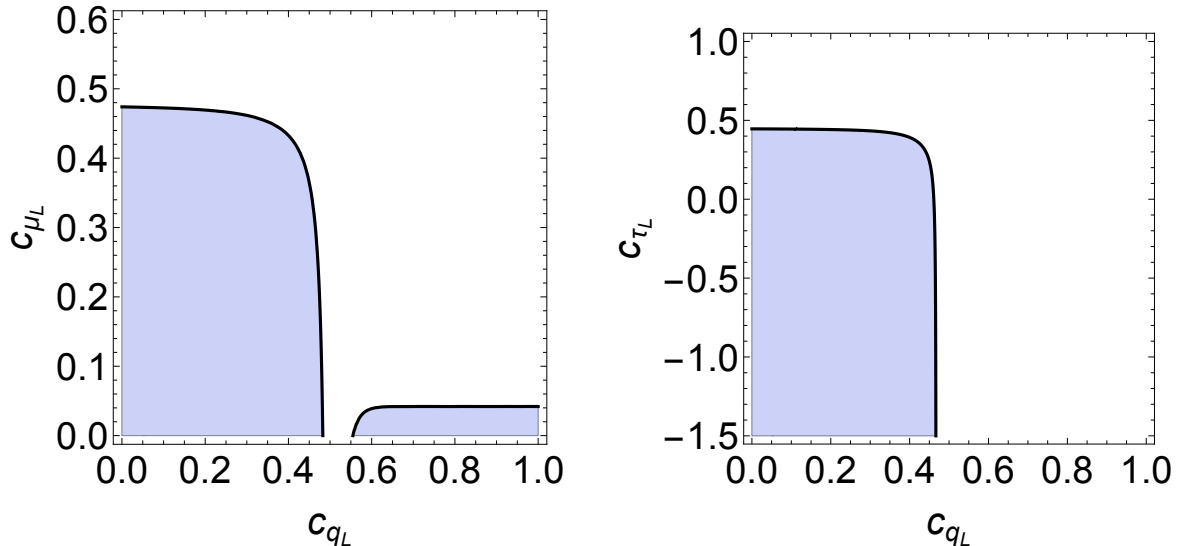


Figure 10: Exclusion region in the plane $(c_{q_L}, c_{\mu_L, \tau_L})$ coming from the searches of massive resonances decaying into di-muons $A_\mu < 0.003$ (left panel), and decaying into di-taus $A_\tau < 0.022$ (right panel), for $M_n = 2$ TeV. We have used $c_{q_R} = 0.8$, $c_{\mu_R} = 0.65$, $c_{\tau_R} = 0.55$, $c_{b_L} = 0.2$, $c_{b_R} = 0.55$ and $c_{t_R} = 0.45$. In the left panel we have considered $c_{\tau_L} = 0.1$, and in the right panel $c_{\mu_L} = 0.44$.

Note that for values $c_{\mu_L} > 0.474$ and $c_{\tau_L} > 0.446$ there is no bound on c_{q_L} . Alternatively, as we can see from both panels of Fig. 10, for $c_{\mu_L} \gtrsim 0.04$ and any value of c_{τ_L} we obtain the mild bound $c_{q_L} \gtrsim 0.48$. In summary, the constraints on the production of dilepton resonances imply that the first generation of quarks is mostly UV localized (elementary) as expected from their mass spectrum.

4.3 Direct Drell-Yan KK gluon searches

Single KK gluons G_μ^n can be produced at LHC by Drell-Yan processes⁷, and decay into top quarks as in the left panel diagram of Fig. 11. ATLAS and CMS have considered

⁷The vertex GGG^n vanishes by orthonormality of wave functions so that G^n cannot be produced by gluon fusion, unless G^n is emitted by a top-quark loop in which case the production is loop suppressed.

KK-gluon production in Randall-Sundrum theories [1] by the Drell-Yan mechanism. ATLAS [75] uses the formalism in Ref. [76], where they consider $G_{q_{L,R}}^1 \simeq -0.2$, for $(q = u, d, c, s)$, $G_{b_R}^1 \simeq -0.2$, $G_{t_L}^1 \simeq 0.95$ and $G_{t_R}^1 \simeq 1.98$. From data at $\sqrt{s} = 8$ TeV corresponding to an integrated luminosity of 20.3 fb^{-1} they obtain the 95% CL lower bound $M_1^{ATLAS} \gtrsim 2.2 \text{ TeV}$. CMS [77] uses data at $\sqrt{s} = 8$ TeV corresponding to an integrated luminosity of 19.7 fb^{-1} . Using the formalism of Ref. [78], where they consider $G_{q_{L,R}}^1 \simeq -0.2$, for $(q = u, d, c, s)$, $G_{b_R}^1 \simeq -0.2$, $G_{t_L}^1 \simeq 1$ and $G_{t_R}^1 \simeq 5$, they obtain the 95% CL lower bound $M_1^{CMS} \gtrsim 2.5 \text{ TeV}$.

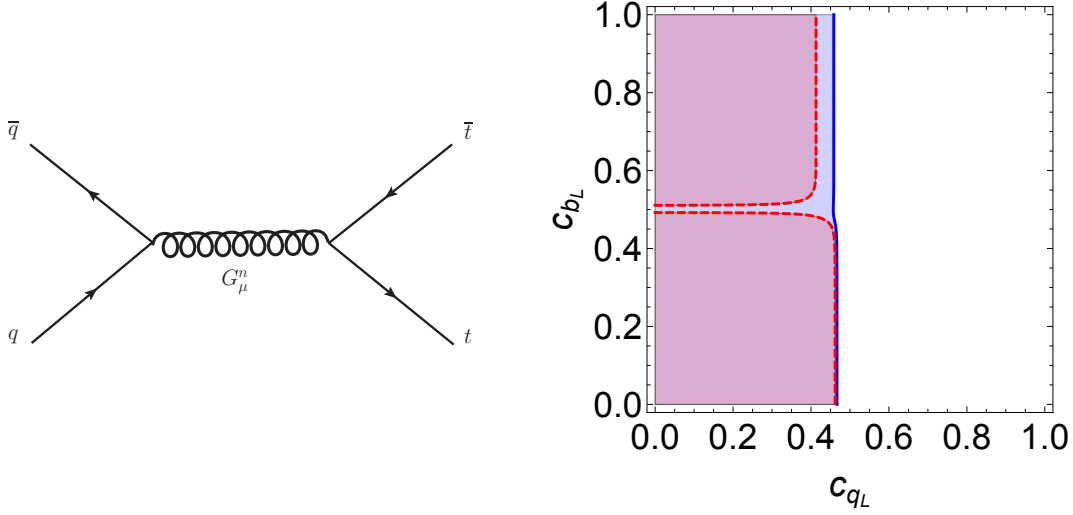


Figure 11: Left panel: Diagrams contributing to the process $\sigma(pp \rightarrow G^n \rightarrow t\bar{t})$. Right panel: Exclusion in the plane (c_{qL}, c_{bL}) coming from ATLAS (red) and CMS (blue) searches of KK gluons decaying into $t\bar{t}$. We have used $c_{qR} = 0.8$, $c_{bR} = 0.55$ and $c_{tR} = 0.45$.

The coupling of the KK-gluon with the fermion f has vector and axial components (unlike the coupling of the gluon zero mode to fermions) and is given by

$$g_{f\bar{f}G_n} = g_s (G_{f_L}^n P_L + G_{f_R}^n P_R) \gamma^\mu t^A \quad (4.7)$$

where g_s is the 4D strong coupling, t^A the $SU(3)$ generators in the triplet representation, $P_{L,R}$ the chirality projectors, and the functions $G_{f_{L,R}}^n$ are defined in Eq. (2.13). Therefore the production cross-section, assuming $c_{u_{L,R}} = c_{d_{L,R}} = c_{c_{L,R}} = c_{s_{L,R}} \equiv c_{q_{L,R}}$, scales as

$$\sigma(pp \rightarrow G_n \rightarrow t\bar{t}) \propto \sum_n \frac{1}{M_n^4} \frac{[(G_{q_L}^n)^2 + (G_{q_R}^n)^2][(G_{t_L}^n)^2 + (G_{t_R}^n)^2]}{\sum_f [(G_{f_L}^n)^2 + (G_{f_R}^n)^2]} \quad (4.8)$$

where the sum over f goes over the three generations of Standard Model quarks, and we are again neglecting the small correction from mixing angles. By comparison with our

model parameters and couplings we can translate the ATLAS and CMS bounds into the exclusion plot in the plane (c_{q_L}, c_{b_L}) , as shown in the right panel of Fig. 11. Notice that given the values of the considered couplings in the ATLAS and CMS models, the CMS bound provides the strongest limit. In particular, and independently of the value of c_{b_L} , searches for KK-gluons lead to the bound $c_{q_L} \gtrsim 0.47$.

4.4 Dimuon resonance from bottom-bottom fusion

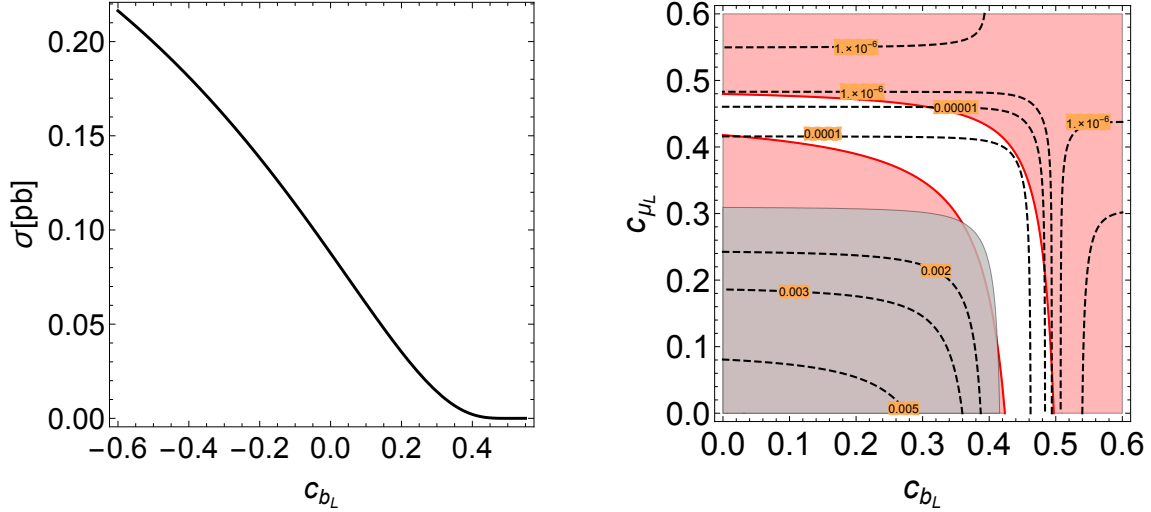


Figure 12: *Left panel: Cross-section production (in pb) in our model for Z^n ($n = 1$) from bottom-bottom fusion in as a function of c_{b_L} . Right panel: Contour plot of $\sigma \cdot \mathcal{B}[Z^n \rightarrow \mu^+ \mu^-]$ for $n = 1$ (in pb) in the plane (c_{b_L}, c_{μ_L}) . We show as a gray band in the bottom part of the figure the experimentally excluded region $\sigma \cdot \mathcal{B} > 10^{-3}$. We overlap as well the allowed region coming from the R_K anomaly. We have considered $c_{\tau_L} = 0.35$.*

In view of the strong constraints imposed by the $R_{K^{(*)}}$ observables on the parameters c_{b_L} and c_{μ_L} , $\mu^+ \mu^-$ production from heavy flavor (bottom) annihilation in the colliding protons ($b\bar{b} \rightarrow \mu^+ \mu^-$) can be sizeable in spite of its suppression by the small PDFs⁸. This issue has been thoroughly analyzed in Refs. [54, 79]. In particular, using the results from Ref. [54] the cross section for Z^n (with $M_n = 2$ TeV, $n = 1$) production from bottom-bottom fusion $\sigma(b\bar{b} \rightarrow Z^1)$ is shown in the left panel of Fig. 12 as a function of c_{b_L} . Contour plots of $\sigma \cdot \mathcal{B}(Z^1 \rightarrow \mu^+ \mu^-)$ are shown in the right panel of Fig. 12. The experimental bounds from the ATLAS dilepton search at $\sqrt{s} = 13$ TeV

⁸In fact we can assume here that, for composite enough b_L quarks, and elementary first and second generation quarks, with $c_{q_{L,R}} \gtrsim 0.5$, bottom-bottom fusion can be dominant over the Drell-Yan mechanism for Z^n production at the LHC.

and 3.2 fb^{-1} [73] for a vector resonance with 2 TeV mass correspond to $\sigma\mathcal{B} \lesssim 10^{-3}$ pb at 95% CL. We can see the corresponding exclusion region in the right panel plot of Fig. 12, which we overlap with the region allowed by the R_K anomaly. As we can see from Fig. 12 most of the space allowed by the R_K anomaly is also allowed by the present LHC bounds on the production of KK Z resonances decaying into dimuons.

4.5 Flavor observables

New physics contributions to $\Delta F = 2$ processes come from the exchange of gluon KK modes. The leading flavor-violating couplings of the KK gluons $G_{n\mu}^A$ involving the down quarks are given by

$$\begin{aligned} \mathcal{L}_s = & g_s G_{n\mu}^A \left[\bar{d}_i \gamma^\mu t_A \left\{ (V_{d_L}^*)_{3i} (V_{d_L})_{3j} (G_{b_L}^n - G_{q_L}^n) P_L \right. \right. \\ & \left. \left. + (V_{d_R}^*)_{3i} (V_{d_R})_{3j} (G_{b_R}^n - G_{q_R}^n) P_R \right\} d_j + \text{h.c.} \right], \end{aligned} \quad (4.9)$$

where t_A are the $SU(3)$ generators in the triplet representation. After integrating out the massive KK gluons, the couplings in Eq. (4.9) give rise to the following set of $\Delta F = 2$ dimension-six operators [16]

$$\begin{aligned} \mathcal{L}_{\Delta F=2} = & \sum_n \left\{ \frac{c_{dij}^{LL(n)}}{M_n^2} (\bar{d}_{iL} \gamma^\mu d_{jL}) (\bar{d}_{iL} \gamma_\mu d_{jL}) + \frac{c_{dij}^{RR(n)}}{M_n^2} (\bar{d}_{iR} \gamma^\mu d_{jR}) (\bar{d}_{iR} \gamma_\mu d_{jR}) \right. \\ & \left. + \frac{c_{dij}^{LR(n)}}{M_n^2} (\bar{d}_{iR} d_{jL}) (\bar{d}_{iL} d_{jR}) \right\}, \end{aligned} \quad (4.10)$$

where

$$\begin{aligned} c_{dij}^{LL,RR(n)} &= \frac{g_s^2}{6} [(V_{d_L}^*)_{3i} (V_{d_L})_{3j}]^2 (G_{b_{L,R}}^n - G_{q_{L,R}}^n)^2, \\ c_{dij}^{LR(n)} &= g_s^2 [(V_{d_L}^*)_{3i} (V_{d_L})_{3j}] [(V_{d_R}^*)_{3i} (V_{d_R})_{3j}] (G_{b_L}^n - G_{q_L}^n) (G_{b_R}^n - G_{q_R}^n). \end{aligned} \quad (4.11)$$

We will assume for the matrices V_{d_R} and V_{u_R} the same structure as for the matrices V_{d_L} and V_{u_L} , respectively. The strongest current bounds on the $\Delta F = 2$ operators come from the operators $(\bar{s}_{L,R} \gamma^\mu d_{L,R})^2$ and $(\bar{s}_R d_L)(\bar{s}_L d_R)$ which contribute to the observables Δm_K and ϵ_K respectively [80]. For the matrix configuration of Eqs. (2.4) and (2.5) the

experimental bounds on Δm_K and ϵ_K can be translated into the constraints

$$\sum_n \frac{(G_{b_{L,R}}^n - G_{q_{L,R}}^n)^2}{M_n^2 [\text{TeV}]} \leq \frac{1.8}{\lambda_0^2 (1-r)^4 |(1-\rho_0)^2 - \eta_0^2|}, \quad (4.12)$$

$$\sum_n \frac{(G_{b_L}^n - G_{q_L}^n)(G_{b_R}^n - G_{q_R}^n)}{M_n^2 [\text{TeV}]} \leq \frac{0.0023}{\lambda_0^2 (1-r)^4 |(1-\rho_0)^2 - \eta_0^2|}, \quad (4.13)$$

$$\sum_n \frac{(G_{b_{L,R}}^n - G_{q_{L,R}}^n)^2}{M_n^2 [\text{TeV}]} \leq \frac{0.0034}{\eta_0 \lambda_0^2 (1-r)^4 |1-\rho_0|}, \quad (4.14)$$

$$\sum_n \frac{(G_{b_L}^n - G_{q_L}^n)(G_{b_R}^n - G_{q_R}^n)}{M_n^2 [\text{TeV}]} \leq \frac{4.3 \times 10^{-6}}{\eta_0 \lambda_0^2 (1-r)^4 |1-\rho_0|}, \quad (4.15)$$

corresponding to the constraints on $\text{Re } c_{d21}^{LL,RR(n)}$, $\text{Re } c_{d21}^{LR(n)}$, $\text{Im } c_{d21}^{LL,RR(n)}$ and $\text{Im } c_{d21}^{LR(n)}$ respectively. We display in the left panel of Fig. 13 these constraints in the plane (c_{b_L}, c_{b_R}) . We have considered for the parameters λ_0 , η_0 and ρ_0 the values

$$\lambda_0 = \lambda, \quad \rho_0 = 0.5, \quad \eta_0 = \eta, \quad (4.16)$$

although other choices would lead to similar constraints. We display as the green shaded region the constraint from Eq. (4.15). The constraints from Eqs. (4.12)-(4.14) are outside the plot range and thus do not interfere with the available region. In this analysis we are taking $c_{q_{L,R}} = 0.8$. The white region is where the flavor bounds from Eqs. (4.12)-(4.15) are satisfied, and the bottom mass can be fixed with a 5D Yukawa coupling $\sqrt{k}\hat{Y}_b \lesssim 4$.

Moreover, flavor-violating couplings of the KK gluons $G_{n\mu}^A$ involving the up-type quarks are similarly given by

$$\begin{aligned} \mathcal{L}_s = & g_s G_{n\mu}^A \left[\bar{u}_i \gamma^\mu t_A \{ (V_{u_L}^*)_{3i} (V_{u_L})_{3j} (G_{t_L}^n - G_{q_L}^n) P_L \right. \\ & \left. + (V_{u_R}^*)_{3i} (V_{u_R})_{3j} (G_{t_R}^n - G_{q_R}^n) P_R \} u_j + \text{h.c.} \right]. \end{aligned} \quad (4.17)$$

After integrating out the KK gluons, operators as $(\bar{c}_{L,R} \gamma^\mu u_{L,R})^2$ and $(\bar{c}_R u_L)(\bar{c}_L u_R)$, which contribute to the observables Δm_D and ϕ_D [80], are generated with Wilson coefficients

$$\begin{aligned} c_{uij}^{LL,RR(n)} &= \frac{g_s^2}{6} [(V_{u_L}^*)_{3i} (V_{u_L})_{3j}]^2 (G_{t_{L,R}}^n - G_{q_{L,R}}^n)^2, \\ c_{uij}^{LR(n)} &= g_s^2 [(V_{u_L}^*)_{3i} (V_{u_L})_{3j}] [(V_{u_R}^*)_{3i} (V_{u_R})_{3j}] (G_{t_L}^n - G_{q_L}^n) (G_{t_R}^n - G_{q_R}^n). \end{aligned} \quad (4.18)$$

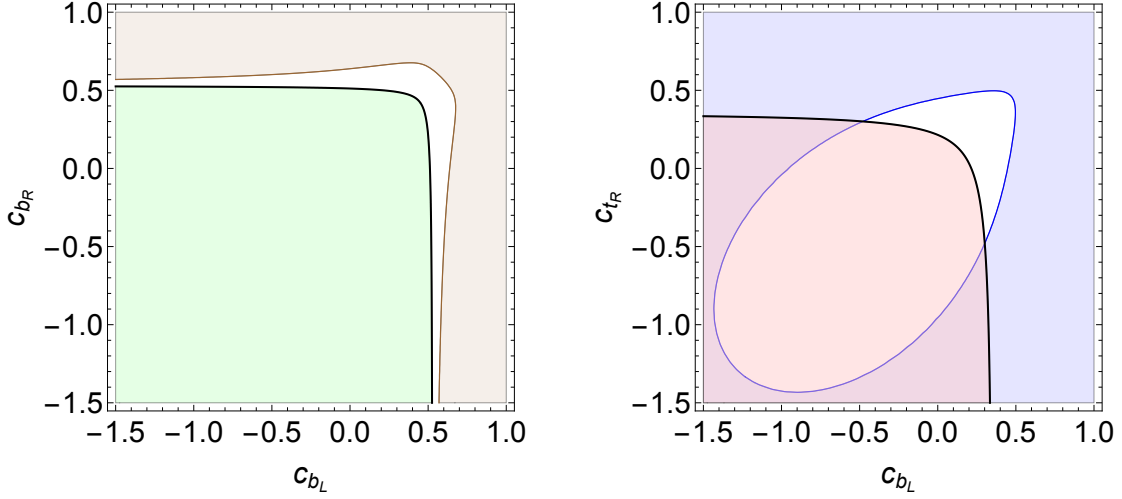


Figure 13: Left panel: Region in the plane (c_{b_L}, c_{b_R}) compatible with the flavor constraints for down-type quarks, Eqs. (4.12)-(4.15), and the value of the bottom quark mass for $\sqrt{k}\hat{Y}_b < 4$. Green region represents the excluded regime from the constraint (4.15). Right panel: Region in the plane (c_{b_L}, c_{t_R}) compatible with the flavor constraints for up-type quarks, Eqs. (4.19)-(4.20), and top quark mass for $\sqrt{k}\hat{Y}_t < 4$. Red region represents the excluded regime from the constraint of the second equation in (4.19).

By again assuming that V_{u_R} has the same structure as V_{u_L} , the experimental data translate into the bounds

$$\sum_n \frac{(G_{t_{L,R}}^n - G_{q_{L,R}}^n)^2}{M_n^2[\text{TeV}]} \leq \frac{22.1}{r^2 F}, \quad \sum_n \frac{(G_{t_L}^n - G_{q_L}^n)(G_{t_R}^n - G_{q_R}^n)}{M_n^2[\text{TeV}]} \leq \frac{0.375}{r^2 F}, \quad (4.19)$$

$$\sum_n \frac{(G_{t_{L,R}}^n - G_{q_{L,R}}^n)^2}{M_n^2[\text{TeV}]} \leq \frac{1.97}{r^2 G}, \quad \sum_n \frac{(G_{t_L}^n - G_{q_L}^n)(G_{t_R}^n - G_{q_R}^n)}{M_n^2[\text{TeV}]} \leq \frac{0.036}{r^2 G}, \quad (4.20)$$

corresponding to the constraints on $\text{Re } c_{u21}^{LL,RR(n)}$ and $\text{Re } c_{u21}^{LR(n)}$ in Eq. (4.19), and $\text{Im } c_{u21}^{LL,RR(n)}$ and $\text{Im } c_{u21}^{LR(n)}$ in Eq. (4.20), respectively. In these equations the functions F and G are

defined by

$$F = \left| (1-r)^2 \left[\left(1 - \frac{\lambda_0}{\lambda} (1 - \rho_0) \right)^2 - \left(\frac{\lambda_0}{\lambda} \eta_0 \right)^2 \right] + 2(1-r) \left[\eta_0 \eta \frac{\lambda_0}{\lambda} - \rho \left(1 - \frac{\lambda_0}{\lambda} (1 - \rho_0) \right) \right] + \rho^2 - \eta^2 \right| \quad (4.21)$$

$$G = \left| (1-r)^2 \eta_0 \frac{\lambda_0}{\lambda} \left[1 - \frac{\lambda_0}{\lambda} (1 - \rho_0) \right] - (1-r) \left[\eta \left(1 + \frac{\lambda_0}{\lambda} (-1 + \rho_0) \right) + \eta_0 \frac{\lambda_0}{\lambda} \rho \right] + \eta \rho \right|. \quad (4.22)$$

We show in the right panel of Fig. 13 these constraints in the plane (c_{b_L}, c_{t_R}) for $r = 0.75$ and the values of λ_0 , ρ_0 and η_0 from Eq. (4.16). The constraints from the first Eq. (4.19) and Eqs. (4.20) are out of the plot range in this case. The white area is the region that can accommodate the top quark mass for 5D Yukawa couplings $\sqrt{k}\hat{Y}_t \lesssim 4$.

5 The $b \rightarrow s\nu\bar{\nu}$ and $b \rightarrow s\tau\tau$ modes

If there is a contribution to the process $\bar{B} \rightarrow \bar{K}\mu\mu$, contributions to the processes $\bar{B} \rightarrow \bar{K}\tau\tau$ and $\bar{B} \rightarrow \bar{K}\nu\bar{\nu}$ will also be generated. We will start by considering the process $\bar{B} \rightarrow \bar{K}\nu\bar{\nu}$ and define

$$R_K^\nu = \frac{\mathcal{B}(\bar{B} \rightarrow \bar{K}\nu\bar{\nu})}{\mathcal{B}(\bar{B} \rightarrow \bar{K}\nu\bar{\nu})_{\text{SM}}}. \quad (5.1)$$

This process is encoded by the effective operators

$$\begin{aligned} \mathcal{O}_\nu^{ij} &= (\bar{s}_L \gamma^\mu b_L) (\bar{\nu}^i \gamma_\mu (1 - \gamma_5) \nu^j), \\ \mathcal{O}_\nu'^{ij} &= (\bar{s}_R \gamma^\mu b_R) (\bar{\nu}^i \gamma_\mu (1 - \gamma_5) \nu^j), \end{aligned} \quad (5.2)$$

generated by the Lagrangian

$$\mathcal{L} = \frac{g}{4c_W} Z_\mu^n \bar{\nu} U^\dagger \gamma_\mu (1 - \gamma_5) G^n U \nu, \quad (5.3)$$

where U is the Pontecorvo-Maki-Nakagawa-Sakata (PMNS) matrix [15] and $G^n = \text{diag}(G_{e_L}^n, G_{\mu_L}^n, G_{\tau_L}^n)$. By defining the Wilson coefficients

$$\Delta C_\nu^{(\prime)ij} = \Delta C_\nu^{(\prime)} (U^\dagger G^n U)^{ij} \quad (5.4)$$

where

$$\Delta C_\nu^{(\prime)} = - \frac{(1-r)\pi g^2 (g_{b_{L(R)}}^{Z_n} - g_{s_{L(R)}}^{Z_n})}{2\sqrt{2}G_F \alpha c_W^2 M_n^2}, \quad (5.5)$$

we can write

$$R_K^\nu = \frac{\sum_\ell |C_\nu^{\text{SM}} + (\Delta C_\nu + \Delta C'_\nu) G_{\ell_L}^n|^2}{3|C_\nu^{\text{SM}}|^2} \quad (5.6)$$

where $C_\nu^{\text{SM}} = -6.4$. The present experimental bound on the branching ratio is $\mathcal{B}(\bar{B} \rightarrow \bar{K} \nu \bar{\nu}) < 3.2 \times 10^{-5}$ [81] at 90% CL, while the Standard Model prediction is $\mathcal{B}(\bar{B} \rightarrow \bar{K} \nu \bar{\nu})_{\text{SM}} = (4.5 \pm 0.7) \times 10^{-6}$. This yields $R_K^\nu < 7.11$ at 90% CL. In the left panel of

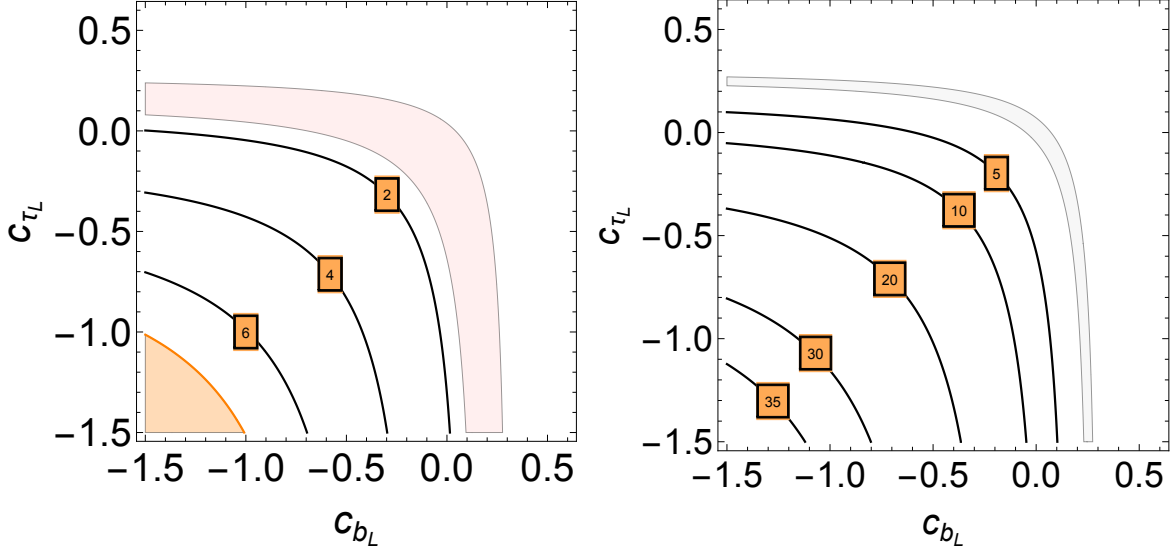


Figure 14: Left panel: Region in the plane (c_{b_L}, c_{τ_L}) that accommodates $R_K^\nu < 7.11$ (orange region is the excluded regime). We also display as a red band the interval $0.7 < R_K^\nu < 1.5$, which is a region close to the SM value, and as solid lines the values $R_K^\nu = 2, 4, 6$. Right panel: Branching ratio R_K^τ in the plane (c_{b_L}, c_{τ_L}) . The gray band corresponds to the interval $0.7 < R_K^\tau < 1.5$, which is a region close to the SM value, and the solid lines are the values of R_K^τ from 5 to 35. We have considered $r = 0.75$ and $c_{\mu_L} = 0.44$.

Fig. 14 we show the prediction of R_K^ν in the plane (c_{b_L}, c_{τ_L}) in our model for $r = 0.75$. The orange shadowed region is excluded at 90% CL. The red band is the region for the interval $0.7 < R_K^\nu < 1.5$, corresponding to a possible future measurement of the observable R_K^ν close to its Standard Model prediction. Moreover a measurement of R_K^ν much larger than the Standard Model prediction would still be possible and be a smoking gun for the model.

Finally, the branching fraction $\mathcal{B}(\bar{B} \rightarrow \bar{K} \tau \tau)$, in particular the ratio

$$R_K^\tau = \frac{\mathcal{B}(\bar{B} \rightarrow \bar{K} \tau \tau)}{\mathcal{B}(\bar{B} \rightarrow \bar{K} \tau \tau)_{\text{SM}}} = \frac{|C_9^{\text{SM}} + \Delta C_9^\tau + \Delta C_9^{\prime\tau}|^2 + |C_{10}^{\text{SM}} + \Delta C_{10}^\tau + \Delta C_{10}^{\prime\tau}|^2}{2|C_9^{\text{SM}}|^2} \quad (5.7)$$

could also be the smoking gun for our model. It has been recently measured by the BaBar Collaboration providing the 90% CL bound $\mathcal{B}(\bar{B} \rightarrow \bar{K} \tau \tau) < 2.25 \times 10^{-3}$ [82],

much larger than the Standard Model prediction $\mathcal{B}(\bar{B} \rightarrow \bar{K}\tau\tau)_{\text{SM}} = (1.44 \pm 0.15) \times 10^{-7}$ [83], and thus leading to the mild bound $R_K^\tau < 1.6 \times 10^4$. Even the future sensitivity of Belle II $\mathcal{B}(\bar{B} \rightarrow \bar{K}\tau\tau) < 2 \times 10^{-4}$ [46] seems to be far away from the Standard Model value. In the right panel of Fig. 14 we show, in the plane (c_{b_L}, c_{τ_L}) , contour plots of the ratio R_K^τ . As we can see the expected Belle II range will not interfere with the allowed region. The gray band corresponds to the interval $0.7 < R_K^\tau < 1.5$ corresponding to a possible future measurement of R_K^τ close to its Standard Model prediction. Again a hypothetical measurement of R_K^τ much larger than the Standard Model prediction would still be possible.

6 Lepton-flavor universality violation in $R_{D^{(*)}}$

The charged current decays $\bar{B} \rightarrow D^{(*)}\ell^-\bar{\nu}_\ell$ have been measured by the BaBar [17, 18], Belle [19–22] and LHCb [23] Collaborations. In particular they measure the quantities

$$R_{D^{(*)}} \equiv R_{D^{(*)}}^{\tau/\ell} = \frac{\mathcal{B}(\bar{B} \rightarrow D^{(*)}\tau^-\bar{\nu}_\tau)}{\mathcal{B}(\bar{B} \rightarrow D^{(*)}\ell^-\bar{\nu}_\ell)} \quad (\ell = \mu \text{ or } e), \quad (6.1)$$

with the experimental result [84, 85]

$$R_D^{\text{exp}} = 0.403 \pm 0.047, \quad R_{D^*}^{\text{exp}} = 0.310 \pm 0.017, \quad \rho = -0.23 \quad (6.2)$$

as averaged by the heavy flavor averaging group (HFAG), which differs from the current Standard Model calculation [84]

$$R_D^{\text{SM}} = 0.300 \pm 0.011, \quad R_{D^*}^{\text{SM}} = 0.254 \pm 0.004 \quad (6.3)$$

by 2.2σ and 3.3σ , respectively, although the combined deviation is $\gtrsim 4\sigma$. This is exhibited in the plot of Fig. 15 where we show, in the plane (R_D, R_{D^*}) , contour lines of 1σ (solid), 2σ (dashed), 3σ (dot-dashed) and 4σ (dotted), as well as the spot with the Standard Model prediction.

The 4D charged current interaction Lagrangian of the KK modes $W_\mu^{(n)}$ with quarks and leptons can be written, in the mass eigenstate basis, as

$$\begin{aligned} \mathcal{L} = & \frac{g}{\sqrt{2}} \sum_n W_\mu^{(n)} \bar{u}_i \left[G_{d_{i_L}}^n V_{ik} + (V_{u_L}^\dagger)_{ij} (G_{d_{j_L}}^n - G_{d_{i_L}}^n) (V_{d_L})_{jk} \right] \gamma^\mu P_L d_k \\ & + \frac{g}{\sqrt{2}} \sum_n W_\mu^{(n)} \bar{\ell}_i G_{\ell_{i_L}}^n U_{ij} \gamma^\mu P_L \nu_j, \end{aligned} \quad (6.4)$$

where i, j, \dots are flavor indices, and V_{u_L} (V_{d_L}) is the unitary matrix diagonalizing the up (down) quark mass matrix⁹.

⁹To prevent lepton flavor violation in our theory, we are assuming that the 5D Yukawa couplings \hat{Y}_ℓ are such that the charged leptons are diagonal in the interaction basis, so that $V_{\ell_{L,R}} \simeq 1$.

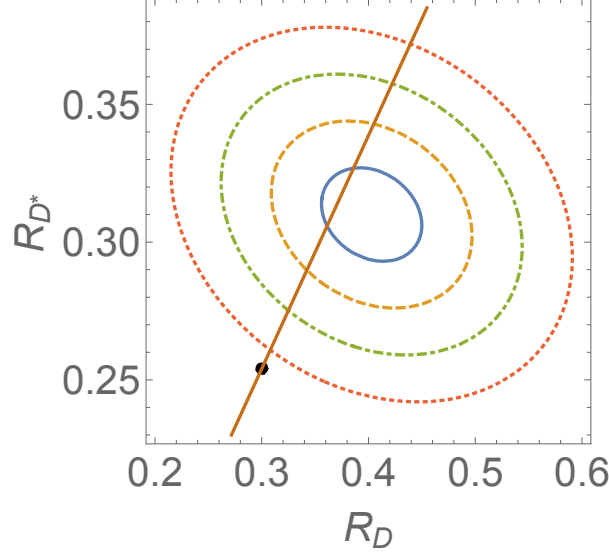


Figure 15: *Experimental region in the (R_D, R_{D^*}) plane from 1σ (inner ellipse)– 4σ (outer ellipse). The black spot is the Standard Model prediction. The straight line is where our model prediction lies.*

After integrating out the KK modes $W^{(n)}$ one obtains the effective Lagrangian

$$\mathcal{L}_{eff} = -\frac{4G_F}{\sqrt{2}} V_{cb} \sum_n [C_n^\tau (\bar{c}\gamma^\nu P_L b) \bar{\tau}\gamma_\nu (U\nu)_\tau + C_n^\mu (\bar{c}\gamma^\nu P_L b) \bar{\mu}\gamma_\nu (U\nu)_\mu] \quad (6.5)$$

where the Wilson coefficients $C_n^{\tau,\mu}$ are given by

$$C_n^{\tau,\mu} = \frac{m_W^2}{m_{W^{(n)}}^2} \left[G_{s_L}^n + \frac{(V_{u_L}^\dagger)_{21}(V_{d_L})_{13}}{V_{cb}} (G_{d_L}^n - G_{s_L}^n) + \frac{(V_{u_L}^\dagger)_{23}(V_{d_L})_{33}}{V_{cb}} (G_{b_L}^n - G_{s_L}^n) \right] G_{\tau_L, \mu_L}^n. \quad (6.6)$$

In case the first and second generation quarks respect the universality condition, the Wilson coefficients can be written as

$$C_n^{\tau,\mu} = \frac{m_W^2}{m_{W^{(n)}}^2} [G_{q_L}^n + r(G_{b_L}^n - G_{q_L}^n)] G_{\tau_L, \mu_L}^n \quad (6.7)$$

and the coefficient r is given by the ratio

$$r = \frac{(V_{u_L}^*)_{32}(V_{d_L})_{33}}{V_{cb}}. \quad (6.8)$$

The corrections to the $R_{D^{(*)}}$ observables from the effective operators are given, in

terms of the Wilson coefficients, as [46]¹⁰

$$R_{D^{(*)}}(C^\tau, C^\mu) = 2R_{D^{(*)}}^{\text{SM}} \frac{|1 + C^\tau|^2}{1 + |1 + C^\mu|^2} . \quad (6.9)$$

This gives the model prediction along the straight line in Fig. 15. Eq. (6.9) translates

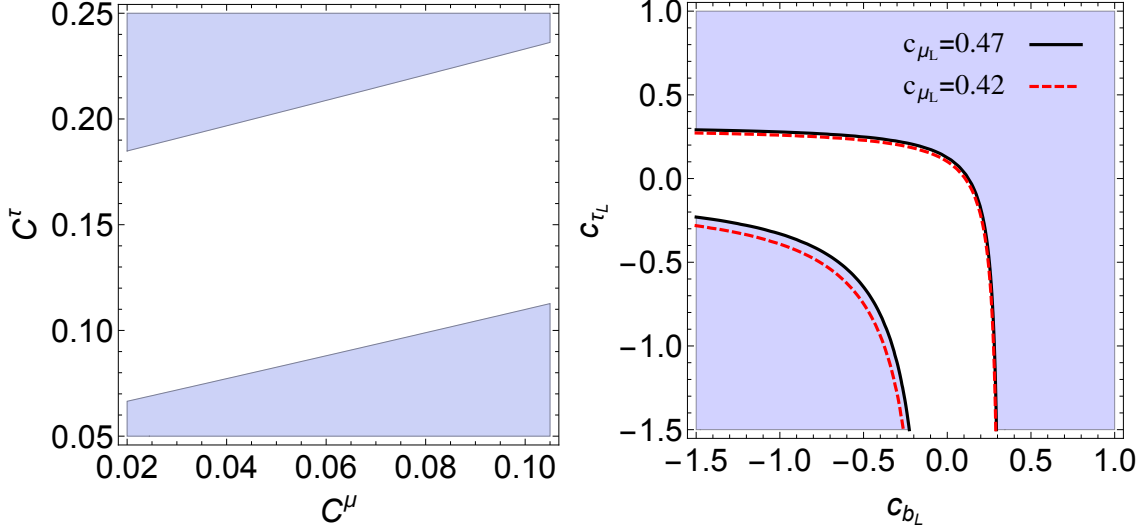


Figure 16: Left panel: Allowed region in the plane (C^μ, C^τ) at the 95% CL. Right panel: Corresponding allowed region in the (c_{b_L}, c_{τ_L}) plane at the 95% CL coming from the (R_D, R_{D^*}) observables. We have considered $c_{\mu_L} = 0.47$ (black lines and shaded area). We also display the limit of the allowed region for the case $c_{\mu_L} = 0.42$ (dashed red lines). We have considered $r = 0.75$, $m_{KK} = 2$ TeV, and $c_{q_L} = 0.8$.

into the allowed region at the 95% CL shown in the left panel of Fig. 16.

The relevant functions in the definition of $C^{\tau, \mu}$, G_{b_L} , G_{τ_L} and G_{μ_L} , depend on the three constants c_{b_L} , c_{τ_L} , c_{μ_L} , which in turn determine the localization of the third generation left-handed quark doublet and third and second generation of left-handed lepton doublets, respectively. Therefore using Eq. (6.9) we get that the model predictions for $R_{D^{(*)}}$ do depend on the constants c_{b_L} , c_{τ_L} , c_{μ_L} . The corresponding 95% CL allowed region in the plane (c_{b_L}, c_{τ_L}) is shown in the right panel of Fig. 16 for the two chosen values $c_{\mu_L} = 0.47, 0.42$. We can see in the plot a mild dependence on the value of the parameter c_{μ_L} . A pretty clear consequence of the plot in the right panel of Fig. 16 is that both b_L and τ_L fermions are localized towards the IR and thus show an important

¹⁰We are keeping here the leading contribution from the first KK mode ($n = 1$) with mass $m_{W^{(1)}} \equiv m_{KK}$ and will suppress the KK-index n . Also notice that the normalization is such that, for the Standard Model, $C_{\text{SM}}^{\tau, \mu} = 1$.

degree of compositeness in the dual theory. In particular we can see that $c_{b_L} \lesssim 0.29$ and $c_{\tau_L} \lesssim 0.29$. Notice that there is no problem to adjust their masses, for $\mathcal{O}(1)$ values of the (dimensionless) 5D Yukawa couplings $\sqrt{k}\hat{Y}_{b,\tau}$, provided that their right-handed partners b_R and τ_R are mostly elementary fermions and thus localized towards the UV brane, as we are assuming in this paper.

6.1 Ditau resonance from bottom-bottom fusion

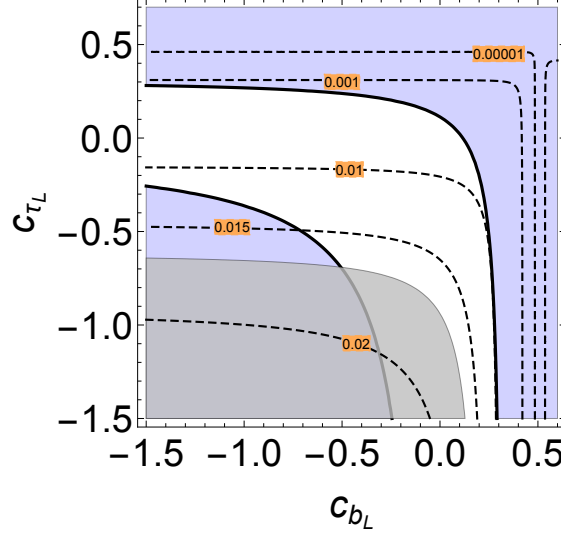


Figure 17: Contour plot of $\sigma \cdot \mathcal{B}[Z^n \rightarrow \tau^+ \tau^-]$ for $n = 1$ (in pb) in the plane (c_{b_L}, c_{τ_L}) . We show as a gray band in the bottom part of the figure the experimentally excluded region $\sigma \cdot \mathcal{B} > 0.017$. We overlap as well the allowed region coming from the (R_D, R_{D^*}) observables. We have considered $c_{\mu_L} = 0.44$.

The strong constraints imposed by the $R_{D^{(*)}}$ observables on the parameters (c_{b_L}, c_{τ_L}) make the $pp \rightarrow \tau\tau$ production from bottom-bottom fusion (especially for IR localized left-handed bottom quarks and UV localized first and second generation quarks) relevant in spite of the suppression of heavy flavors in PDFs. The analysis has been done in Ref. [54] and we will follow here the same lines as for the dimuon production from bottom-bottom fusion, as constrained by the R_K anomaly. The cross-section for production of $b\bar{b} \rightarrow Z^1$ is given by the plot in the left panel of Fig. 12. Using this information we show in the plot of Fig. 17 contour lines of $\sigma \cdot \mathcal{B}(Z^1 \rightarrow \tau\tau)$. The bounds from the CMS ditau searches at $\sqrt{s} = 13$ TeV and 2.2 fb^{-1} [74] yield for a 2 TeV vector resonance the 95% CL bound $\sigma \mathcal{B}(Z^1 \rightarrow \tau\tau) \lesssim 0.017$ pb. The corresponding excluded region (the grey area) is shown, in the (c_{b_L}, c_{τ_L}) plane, in the plot of Fig. 17 which we overlap with the allowed region by the $R_{D^{(*)}}$ anomaly. As we can see part

of (but not all) the region allowed by $R_{D^{(*)}}$ (the part of the parameter region where b_L and/or τ_L are mostly localized toward the IR) is already excluded by LHC data on ditau production. However the most interesting region, where $c_{\tau_L} > c_{b_L}$, is entirely allowed.

6.2 Lepton flavor universality tests

The anomaly on the experimental values of $R_{D^{(*)}}^{\tau/\ell}$ also has to be contrasted with the non-observation of flavor universality violation effects in the μ/e sector and with lepton flavor universality tests in tau decays¹¹. In particular in the μ/e sector, the non-observation of flavor universality violation at the 2% level translates into the condition $R_{D^{(*)}}^{\mu/e} \lesssim 1.02$ [51, 55], with

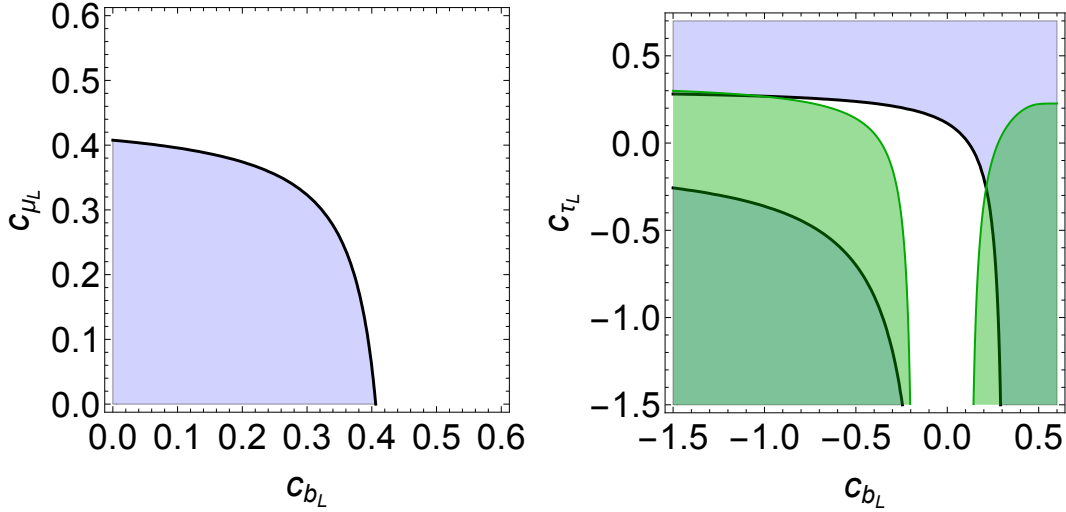


Figure 18: Left panel: Exclusion (shadowed) region in the plane (c_{b_L}, c_{μ_L}) by the condition $R_{D^{(*)}}^{\mu/e} \lesssim 1.02$. Right panel: We display in green the excluded region corresponding to $R_{\tau}^{\tau/\mu} \in [0.996, 1.008]$ in the plane (c_{b_L}, c_{τ_L}) . We overlap as well the allowed region coming from the (R_D, R_{D^*}) observables. We have considered $c_{\mu_L} = 0.44$. We have used in both plots $r = 0.75$ and $m_{KK} = 2$ TeV.

$$R_{D^{(*)}}^{\mu/e} = \frac{\mathcal{B}(\overline{B} \rightarrow D^{(*)} \mu^- \overline{\nu}_\mu)}{\mathcal{B}(\overline{B} \rightarrow D^{(*)} e^- \overline{\nu}_e)} = |1 + C^\mu|^2 \quad (6.10)$$

where we have assumed that $c_{e_L} = 0.5$ and so $C^e = 0$. Consequently the condition $R_{D^{(*)}}^{\mu/e} \lesssim 1.02$ translates into $C^\mu \lesssim 0.010$. As C^μ is a function of (c_{b_L}, c_{μ_L}) we plot in the

¹¹We thank Paride Paradisi for pointing out the corresponding observables, which were missing from the first version of the paper, to us.

left panel of Fig. 18 the exclusion condition which corresponds to the shadowed area. As we can see from the right plot of Fig. 16, and the left panel of Fig. 18, the bound $c_{b_L} \lesssim 0.29$ would translate into the bound $c_{\mu_L} \gtrsim 0.33$ which is perfectly consistent with the amount of lepton flavor universality breaking obtained in this paper.

Finally the $R_{D^{(*)}}$ anomaly, and its corresponding lepton flavor universality violation in the τ/μ sector, also has to agree with flavor universality tests performed at the per mille level in tau decays. In particular the observables

$$R_\tau^{\tau/\ell} = \frac{\mathcal{B}(\tau \rightarrow \ell \nu \bar{\nu})/\mathcal{B}(\tau \rightarrow \ell \nu \bar{\nu})_{\text{SM}}}{\mathcal{B}(\mu \rightarrow e \nu \bar{\nu})/\mathcal{B}(\mu \rightarrow e \nu \bar{\nu})_{\text{SM}}}, \quad (\ell = \mu, e) \quad (6.11)$$

are subject to the experimental bounds [55, 86], $R_\tau^{\tau/\mu} \in [0.996, 1.008]$ and $R_\tau^{\tau/e} \in [1.000, 1.012]$ at 95% CL. In our model, fixing $c_{e_L} = 0.5$ implies that $R_\tau^{\tau/e} = 1$ while, including the relevant one-loop radiative corrections [55], we can write the $R_\tau^{\tau/\mu}$ observable as

$$R_\tau^{\tau/\mu} = 1 + 2 \frac{m_W^2}{m_{W^{(n)}}^2} G_{\tau_L}^n (G_{\mu_L}^n - 0.065 G_{b_L}^n). \quad (6.12)$$

One can see that radiative effects proportional to $G_{b_L}^n$ (coming from closing the $b \bar{c}$ quark line which contributes to $R_{D^{(*)}}$ by emitting a W -gauge boson) with loop suppression factors, compete with tree-level effects proportional to $G_{\mu_L}^n$, as accommodation of the $R_{D^{(*)}}$ anomaly implies $G_{b_L}^n \gg G_{\mu_L}^n$. This competition produces a partial cancellation and the result leaves more available space than any of the individual effects¹², without introducing any fine-tuning. The allowed region in the plane (c_{b_L}, c_{τ_L}) is shown in the right panel of Fig. 18. The green region is excluded from Eq. (6.12) for $c_{\mu_L} = 0.44$, a value consistent with the R_K anomaly from Fig. 5. The plot from the $R_{D^{(*)}}$ anomaly is superimposed and the white region is allowed by both.

The short conclusion in this section is that lepton flavor universality tests can easily agree with the experimental value of the $R_{D^{(*)}}$ anomaly.

6.3 The $Z\bar{\tau}\tau$ coupling

Finally the $R_{D^{(*)}}$ anomaly has to be contrasted with radiative and KK corrections to the $Z\bar{\tau}\tau$ coupling. We will do it following the formalism of Sec. 4.1 and using the experimental value from the fit of Ref. [71]

$$g_{\tau_L}^Z = -0.26930 \pm 0.00058, \quad (6.13)$$

which leads to the result¹³

¹²We thank Paride Paradisi for pointing out this effect to us.

¹³The recent fit from Ref. [72] yields $\Delta g_{\tau_L}^Z + \delta g_{\tau_L}^Z = (0.18 \pm 0.59) \times 10^{-3}$ consistent with Eq. (6.14).

$$\Delta g_{\tau_L}^Z + \delta g_{\tau_L}^Z = (0.09 \pm 0.58) \times 10^{-3}, \quad (6.14)$$

where $\Delta g_{\tau_L}^Z$ is given by Eq. (4.3) and $\delta g_{\tau_L}^Z$ by Eq. (1.7). The allowed region at 2σ is shown in the plot of Fig. 19.

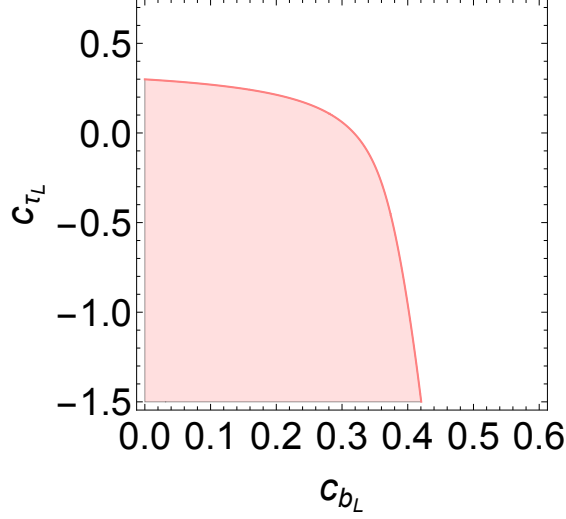


Figure 19: Region at 2σ in the plane (c_{b_L}, c_{τ_L}) that accommodates the constraint $\Delta g_{\tau_L}^Z + \delta g_{\tau_L}^Z$ (white region) as shown in Eq. (6.14).

To conclude this section and as we can see by comparison of Figs. 16 and 19, there is a tension between data from the $R_{D^{(*)}}$ anomaly and electroweak observables, in particular the $Z^\mu \tau_L \gamma_\mu \tau_L$ coupling, $g_{\tau_L}^Z$, because the electroweak corrections to the effective operator $(\bar{t}_L \gamma^\mu t_L)(\bar{\ell}_L \gamma_\mu \ell_L)$, give rise to the operator $(H^\dagger D_\mu H)(\bar{\ell}_L \gamma^\mu \ell_L)$ and thus trigger, after electroweak breaking, a correction to the $Z \bar{\tau}_L \tau_L$ coupling proportional to h_t^2 . In short, assuming a Wolfenstein-like structure for the unitary transformations $V_{u_{L(R)}}, V_{d_{L(R)}}$ [i.e. $r \lesssim 1$ in Eq. (2.4)] we find that the $R_{D^{(*)}}$ anomaly is only satisfied by very composite fermions (b_L, τ_L) which are in tension with the experimental value of $g_{\tau_L}^Z$.

7 Conclusions and outlook

In this paper we have tried to accommodate present data on lepton flavor universality violation in a model with a warped extra dimension, where the Standard Model fields propagate, and which is basically in agreement with electroweak precision observables thanks to a strong deformation of conformality of the metric near the IR brane. Every fermion field $f_{L,R}$ in the model is characterized by a five-dimensional Dirac mass

parametrized by a real constant $c_{f_{L,R}}$ which controls its localization or, equivalently in the dual theory, its degree of compositeness. Fermions with $c_f > 0.5$ ($c_f < 0.5$) are localized toward the UV (IR) brane and correspond in the dual theory to mostly elementary (composite) fields. The coupling of gauge boson KK-modes with fermion f essentially depend on the value of c_f : it is very small for elementary fermions and large for composite fermions. In this way the basic elements of lepton flavor universality violation through the exchange of KK gauge bosons is built in *ab initio*, and controlled in the theory by the different values of c_f . In particular it is very easy to generate lepton flavor universality violation for electrons, muons and taus by just assuming that electrons are elementary fermions while muons and taus have a certain degree of compositeness.

The results in this paper depend, to some extent, on the five-dimensional Yukawa matrices $Y_{u,d}^{5D} \equiv \sqrt{k}\hat{Y}_{u,d}$ which in turn determine, along with the constants $c_{f_{L,R}}$, the unitary transformations $V_{u_{L,R}}$ and $V_{d_{L,R}}$. In the absence of a UV theory for the Yukawa couplings $\hat{Y}_{u,d}$ we have considered arbitrary matrices $V_{u_{L,R}}$ and $V_{d_{L,R}}$ satisfying the Wolfenstein parametrization, and such that $V_{u_L}^\dagger V_{d_L} = V$, the CKM matrix. As those matrices depend on a number of parameters we have considered generic values for their entries, satisfying the Wolfenstein parametrization and leading to strong bounds in the down-quark sector from Δm_K and ϵ_K and in the up-quark sector from Δm_D and ϕ_D . An analysis for different values of the parameters, in case they would be provided by particular UV completions of the present model, should be readily done along similar lines as in the present paper.

Moreover our theory is *lepton flavor conserving*, as we have considered in the charged lepton sector models where the 5D Yukawa matrix \hat{Y}_ℓ is already in diagonal form, i.e. $V_{\ell_{L,R}} = 1_3$, thus avoiding strong constraints from lepton flavor violation. Had we considered models with more generic Wolfenstein-like matrices in the charged lepton sector $V_{\ell_{L,R}}$, bounds on lepton flavor violating processes, as e.g. $\tau \rightarrow 3\mu$ or $\mu \rightarrow e\gamma$, would have imposed very strong constraints on the off-diagonal elements of $V_{\ell_{L,R}}$. We postpone the study of this class of models for future investigation.

Using the above ideas it is straightforward to accommodate the present flavor universality violations in the observables R_K , as well as the rest of observables depending on $b \rightarrow s\ell^+\ell^-$ and $b \rightarrow s\nu\bar{\nu}$, processes. The summary results from R_K are given in the left panel plot of Fig. 20 where we show the allowed regions in the plane (c_{b_L}, c_{μ_L}) , taking into account all different constraints obtained by electroweak observables, direct LHC searches and flavor observables. We also have included the green region which is excluded from Eq. (6.12) for values of c_{τ_L} below the bound in the plot of Fig. 19. All

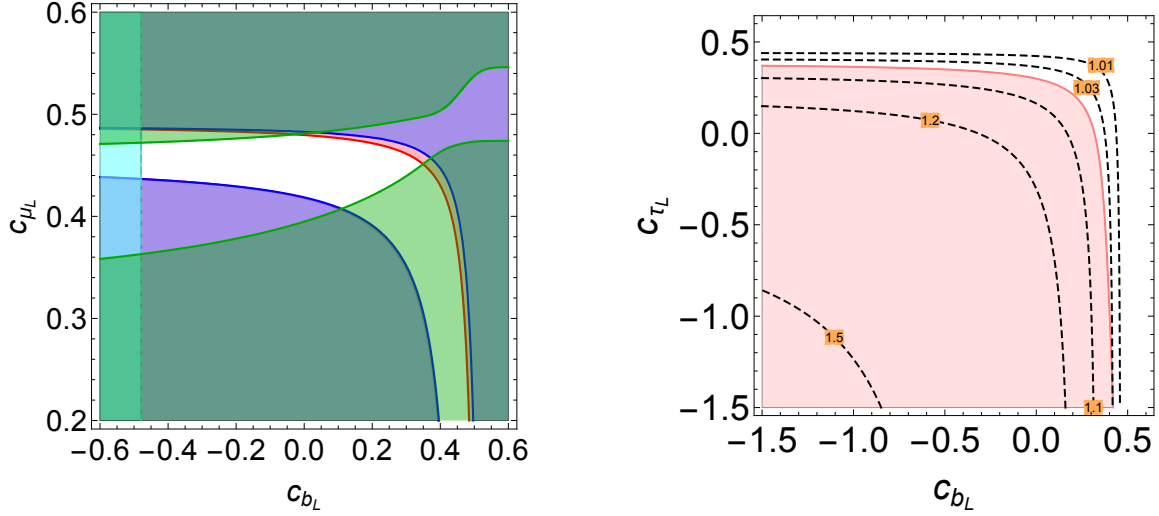


Figure 20: Left panel: Region in the (c_{b_L}, c_{μ_L}) plane that accommodates R_K (solid red line) and R_0 (blue line). We also overlap the flavor constraints region $c_{b_L} > -0.48$. We display as green band the excluded region corresponding to $R_{\tau}^{\tau/\mu}$ [cf. Fig. 18 (right panel)]. The white region is allowed for any value of c_{τ_L} . Right panel: Contour plot in the (c_{b_L}, c_{τ_L}) plane of the $R_{D^{(*)}}/R_{D^{(*)}}^{SM}$. The red shaded area corresponds to the bound from $g_{\tau_L}^Z$ (see Fig. 19).

of them put together leave the approximate allowed region

$$0.41 \lesssim c_{\mu_L} \lesssim 0.48, \quad -0.48 \lesssim c_{b_L} \lesssim 0.35, \quad (7.1)$$

which translate into pretty composite left-handed bottom quarks, and slightly composite left-handed muon leptons. The sequence in Eq. (7.1) is roughly, within factors of $\mathcal{O}(\text{few})$, in agreement with their relative masses, whose absolute values can be easily fixed with appropriate values of the right-handed component parameters, c_{b_R} , and c_{μ_R} , and natural values of the five-dimensional Yukawa couplings.

On the other hand, trying to accommodate the present flavor universality violations in the $R_{D^{(*)}}$ observables generates a tension with electroweak observables, in particular with the $Z^\mu \bar{\tau}_L \gamma_\mu \tau$ coupling as can be seen from the right panel of Fig. 20 where we gather the allowed region by the $g_{\tau_L}^Z$ coupling, and contour plots of the observables $R_{D^{(*)}}/R_{D^{(*)}}^{SM}$ with experimental values

$$\frac{R_D^{\text{exp}}}{R_D^{SM}} = 1.37 \pm 0.17, \quad \frac{R_{D^*}^{\text{exp}}}{R_{D^*}^{SM}} = 1.28 \pm 0.08. \quad (7.2)$$

As we can see from the plot, deviations from one of $R_{D^{(*)}}/R_{D^{(*)}}^{SM}$ are constrained by $g_{\tau_L}^Z$ to values $\lesssim 5\%$. A possible way out is to allow some (small) departure of the matrices V_{d_L} and V_{u_L} from the Wolfenstein pattern, in particular by allowing that

$V_{cb} \ll (V_{u_L})_{32} \ll 1$ which implies in particular that $r \gtrsim 1$. As we can see from Eq. (6.7) this would strengthen the value of $R_{D^{(*)}}$ with less composite τ_L leptons, which in turn unfasten the tension with the experimental value of $g_{\tau_L}^Z$. Of course the price to pay for this “solution” is introducing some degree of fine-tuning for the fixing of the small CKM unitary matrix entries from matrices V_{d_L} and V_{u_L} with larger entries. This *little fine-tuned* solution will be worked out elsewhere.

The remaining lepton-flavor universality violation is the anomalous magnetic moment of the muon $a_\mu = (g_\mu - 2)/2$, which deviates with respect to the Standard Model prediction a_μ^{SM} by $\sim 3.6\sigma$, while the corresponding observable for the electron, a_e , is in very good agreement with the Standard Model. Our theory has the required ingredients to trigger a sizeable correction to the muon anomalous magnetic moment through the mixing (induced by the muon Yukawa coupling) between left and right-handed muon n -KK modes and the corresponding zero modes. However as the mixing is controlled by the experimental bounds $|\delta g_{L,R}/g_{L,R}| \lesssim 10^{-3}$, it does not have enough power to trigger a large effect, and extra physics should be introduced in the model to encompass explanation of anomalous magnetic moment of the muon. In the context of warped theories, a possibility was already presented in Ref. [87] where heavy vector-like leptons, with the quantum numbers of the Standard Model muons, were introduced and conveniently mix with them through appropriate Yukawa couplings. As it was proven in Ref. [87] the explanation of this effect is consistent with all electroweak and flavor observables, and direct searches of heavy leptons, and implies a high degree of compositeness for vector-like leptons which could be detected at present and future colliders.

Acknowledgments

We thank Paride Paradisi for useful observations on the observables $R_{D^{(*)}}^{\mu/e}$ and $R_\tau^{\tau/\ell}$ constraining our model parameters. L.S. is supported by a *Beca Predoctoral Severo Ochoa del Ministerio de Economía y Competitividad* (SVP-2014-068850), and E.M. is supported by the *Universidad del País Vasco UPV/EHU*, Bilbao, Spain, as a Visiting Professor. The work of M.Q. and L.S. is also partly supported by Spanish MINECO under Grant CICYT-FEDER-FPA2014-55613-P, by the Severo Ochoa Excellence Program of MINECO under the grant SO-2012-0234, by *Secretaria d’Universitats i Recerca del Departament d’Economia i Coneixement de la Generalitat de Catalunya* under Grant 2014 SGR 1450, and by the CERCA Program/Generalitat de Catalunya. The research of E.M. is also partly supported by Spanish MINECO under Grant FPA2015-64041-C2-1-P, by the Basque Government under Grant IT979-16, and by the Spanish Consolider Ingenio 2010 Programme CPAN (CSD2007-00042).

References

- [1] L. Randall and R. Sundrum, *A Large mass hierarchy from a small extra dimension*, *Phys. Rev. Lett.* **83** (1999) 3370–3373, [[hep-ph/9905221](#)].
- [2] J. A. Cabrer, G. von Gersdorff and M. Quiros, *Soft-Wall Stabilization*, *New J. Phys.* **12** (2010) 075012, [[0907.5361](#)].
- [3] J. A. Cabrer, G. von Gersdorff and M. Quiros, *Warped Electroweak Breaking Without Custodial Symmetry*, *Phys. Lett.* **B697** (2011) 208–214, [[1011.2205](#)].
- [4] J. A. Cabrer, G. von Gersdorff and M. Quiros, *Suppressing Electroweak Precision Observables in 5D Warped Models*, *JHEP* **05** (2011) 083, [[1103.1388](#)].
- [5] J. A. Cabrer, G. von Gersdorff and M. Quiros, *Improving Naturalness in Warped Models with a Heavy Bulk Higgs Boson*, *Phys. Rev.* **D84** (2011) 035024, [[1104.3149](#)].
- [6] J. A. Cabrer, G. von Gersdorff and M. Quiros, *Warped 5D Standard Model Consistent with EWPT*, *Fortsch. Phys.* **59** (2011) 1135–1138, [[1104.5253](#)].
- [7] A. Carmona, E. Ponton and J. Santiago, *Phenomenology of Non-Custodial Warped Models*, *JHEP* **10** (2011) 137, [[1107.1500](#)].
- [8] J. A. Cabrer, G. von Gersdorff and M. Quiros, *Flavor Phenomenology in General 5D Warped Spaces*, *JHEP* **01** (2012) 033, [[1110.3324](#)].
- [9] M. Quiros, *Higgs Bosons in Extra Dimensions*, *Mod. Phys. Lett.* **A30** (2015) 1540012, [[1311.2824](#)].
- [10] E. Megias, O. Pujolas and M. Quiros, *On dilatons and the LHC diphoton excess*, *JHEP* **05** (2016) 137, [[1512.06106](#)].
- [11] E. Megias, O. Pujolas and M. Quiros, *On light dilaton extensions of the Standard Model*, *EPJ Web Conf.* **126** (2016) 05010, [[1512.06702](#)].
- [12] E. Megias, G. Panico, O. Pujolas and M. Quiros, *Light dilatons in warped space: Higgs boson and LHCb anomalies*, *Nucl. Part. Phys. Proc.* **282-284** (2017) 194–198, [[1609.01881](#)].
- [13] H. Davoudiasl, S. Gopalakrishna, E. Ponton and J. Santiago, *Warped 5-Dimensional Models: Phenomenological Status and Experimental Prospects*, *New J. Phys.* **12** (2010) 075011, [[0908.1968](#)].
- [14] M. E. Peskin and T. Takeuchi, *Estimation of oblique electroweak corrections*, *Phys. Rev.* **D46** (1992) 381–409.
- [15] PARTICLE DATA GROUP collaboration, C. Patrignani et al., *Review of Particle Physics*, *Chin. Phys.* **C40** (2016) 100001.
- [16] E. Megias, G. Panico, O. Pujolas and M. Quiros, *A Natural origin for the LHCb anomalies*, *JHEP* **09** (2016) 118, [[1608.02362](#)].

- [17] BABAR collaboration, J. P. Lees et al., *Evidence for an excess of $\bar{B} \rightarrow D^{(*)}\tau^{-}\bar{\nu}_{\tau}$ decays*, *Phys. Rev. Lett.* **109** (2012) 101802, [[1205.5442](#)].
- [18] BABAR collaboration, J. P. Lees et al., *Measurement of an Excess of $\bar{B} \rightarrow D^{(*)}\tau^{-}\bar{\nu}_{\tau}$ Decays and Implications for Charged Higgs Bosons*, *Phys. Rev.* **D88** (2013) 072012, [[1303.0571](#)].
- [19] BELLE collaboration, M. Huschle et al., *Measurement of the branching ratio of $\bar{B} \rightarrow D^{(*)}\tau^{-}\bar{\nu}_{\tau}$ relative to $\bar{B} \rightarrow D^{(*)}\ell^{-}\bar{\nu}_{\ell}$ decays with hadronic tagging at Belle*, *Phys. Rev.* **D92** (2015) 072014, [[1507.03233](#)].
- [20] BELLE collaboration, Y. Sato et al., *Measurement of the branching ratio of $\bar{B}^0 \rightarrow D^{*+}\tau^{-}\bar{\nu}_{\tau}$ relative to $\bar{B}^0 \rightarrow D^{*+}\ell^{-}\bar{\nu}_{\ell}$ decays with a semileptonic tagging method*, *Phys. Rev.* **D94** (2016) 072007, [[1607.07923](#)].
- [21] A. Abdesselam et al., *Measurement of the τ lepton polarization in the decay $\bar{B} \rightarrow D^{*}\tau^{-}\bar{\nu}_{\tau}$* , [1608.06391](#).
- [22] BELLE collaboration, S. Hirose et al., *Measurement of the τ lepton polarization and $R(D^{*})$ in the decay $\bar{B} \rightarrow D^{*}\tau^{-}\bar{\nu}_{\tau}$* , *Phys. Rev. Lett.* **118** (2017) 211801, [[1612.00529](#)].
- [23] LHCb collaboration, R. Aaij et al., *Measurement of the ratio of branching fractions $\mathcal{B}(\bar{B}^0 \rightarrow D^{*+}\tau^{-}\bar{\nu}_{\tau})/\mathcal{B}(\bar{B}^0 \rightarrow D^{*+}\mu^{-}\bar{\nu}_{\mu})$* , *Phys. Rev. Lett.* **115** (2015) 111803, [[1506.08614](#)].
- [24] LHCb collaboration, R. Aaij et al., *Test of lepton universality using $B^{+} \rightarrow K^{+}\ell^{+}\ell^{-}$ decays*, *Phys. Rev. Lett.* **113** (2014) 151601, [[1406.6482](#)].
- [25] W. Altmannshofer and D. M. Straub, *New Physics in $B \rightarrow K^{*}\mu\mu$?*, *Eur. Phys. J.* **C73** (2013) 2646, [[1308.1501](#)].
- [26] R. Gauld, F. Goertz and U. Haisch, *On minimal Z' explanations of the $B \rightarrow K^{*}\mu^{+}\mu^{-}$ anomaly*, *Phys. Rev.* **D89** (2014) 015005, [[1308.1959](#)].
- [27] D. Aristizabal Sierra, F. Staub and A. Vicente, *Shedding light on the $b \rightarrow s$ anomalies with a dark sector*, *Phys. Rev.* **D92** (2015) 015001, [[1503.06077](#)].
- [28] A. Crivellin, L. Hofer, J. Matias, U. Nierste, S. Pokorski and J. Rosiek, *Lepton-flavour violating B decays in generic Z' models*, *Phys. Rev.* **D92** (2015) 054013, [[1504.07928](#)].
- [29] A. Celis, J. Fuentes-Martin, M. Jung and H. Serodio, *Family nonuniversal Z models with protected flavor-changing interactions*, *Phys. Rev.* **D92** (2015) 015007, [[1505.03079](#)].
- [30] A. Falkowski, M. Nardecchia and R. Ziegler, *Lepton Flavor Non-Universality in B -meson Decays from a $U(2)$ Flavor Model*, *JHEP* **11** (2015) 173, [[1509.01249](#)].
- [31] S. Descotes-Genon, L. Hofer, J. Matias and J. Virto, *Global analysis of $b \rightarrow s\ell\ell$ anomalies*, *JHEP* **06** (2016) 092, [[1510.04239](#)].

- [32] B. Allanach, F. S. Queiroz, A. Strumia and S. Sun, *Z models for the LHCb and $g - 2$ muon anomalies*, *Phys. Rev.* **D93** (2016) 055045, [[1511.07447](#)].
- [33] D. Buttazzo, A. Greljo, G. Isidori and D. Marzocca, *Toward a coherent solution of diphoton and flavor anomalies*, *JHEP* **08** (2016) 035, [[1604.03940](#)].
- [34] P. Biancofiore, P. Colangelo and F. De Fazio, *On the anomalous enhancement observed in $B \rightarrow D^{(*)}\tau\bar{\nu}_\tau$ decays*, *Phys. Rev.* **D87** (2013) 074010, [[1302.1042](#)].
- [35] S. Descotes-Genon, L. Hofer, J. Matias and J. Virto, *The $b \rightarrow sl^+l^-$ anomalies and their implications for new physics*, in *51st Rencontres de Moriond on EW Interactions and Unified Theories La Thuile, Italy, March 12-19, 2016*, 2016. [1605.06059](#).
- [36] N. Kosnik, *Model independent constraints on leptoquarks from $b \rightarrow sl^+\ell^-$ processes*, *Phys. Rev.* **D86** (2012) 055004, [[1206.2970](#)].
- [37] Y. Sakaki, M. Tanaka, A. Tayduganov and R. Watanabe, *Testing leptoquark models in $\bar{B} \rightarrow D^{(*)}\tau\bar{\nu}$* , *Phys. Rev.* **D88** (2013) 094012, [[1309.0301](#)].
- [38] G. Hiller and M. Schmaltz, *R_K and future $b \rightarrow s\ell\ell$ physics beyond the standard model opportunities*, *Phys. Rev.* **D90** (2014) 054014, [[1408.1627](#)].
- [39] B. Gripaios, M. Nardecchia and S. A. Renner, *Composite leptoquarks and anomalies in B-meson decays*, *JHEP* **05** (2015) 006, [[1412.1791](#)].
- [40] S. Sahoo and R. Mohanta, *Scalar leptoquarks and the rare B meson decays*, *Phys. Rev.* **D91** (2015) 094019, [[1501.05193](#)].
- [41] D. Beirevi, S. Fajfer and N. Konik, *Lepton flavor nonuniversality in bs^{+-} processes*, *Phys. Rev.* **D92** (2015) 014016, [[1503.09024](#)].
- [42] R. Alonso, B. Grinstein and J. Martin Camalich, *Lepton universality violation and lepton flavor conservation in B-meson decays*, *JHEP* **10** (2015) 184, [[1505.05164](#)].
- [43] B. Dumont, K. Nishiwaki and R. Watanabe, *LHC constraints and prospects for S_1 scalar leptoquark explaining the $\bar{B} \rightarrow D^{(*)}\tau\bar{\nu}$ anomaly*, *Phys. Rev.* **D94** (2016) 034001, [[1603.05248](#)].
- [44] D. Das, C. Hati, G. Kumar and N. Mahajan, *Towards a unified explanation of $R_{D^{(*)}}$, R_K and $(g - 2)_\mu$ anomalies in a left-right model with leptoquarks*, *Phys. Rev.* **D94** (2016) 055034, [[1605.06313](#)].
- [45] S. Sahoo, R. Mohanta and A. K. Giri, *Explaining the R_K and $R_{D^{(*)}}$ anomalies with vector leptoquarks*, *Phys. Rev.* **D95** (2017) 035027, [[1609.04367](#)].
- [46] B. Bhattacharya, A. Datta, J.-P. Guvin, D. London and R. Watanabe, *Simultaneous Explanation of the R_K and $R_{D^{(*)}}$ Puzzles: a Model Analysis*, *JHEP* **01** (2017) 015, [[1609.09078](#)].

- [47] R. Alonso, B. Grinstein and J. Martin Camalich, *The lifetime of the B_c^- meson and the anomalies in $B \rightarrow D^{(*)}\tau\nu$* , *Phys. Rev. Lett.* **118** (2017) 081802, [[1611.06676](#)].
- [48] A. Celis, M. Jung, X.-Q. Li and A. Pich, *Scalar contributions to $b \rightarrow c(u)\tau\nu$ transitions*, *Phys. Lett.* **B771** (2017) 168–179, [[1612.07757](#)].
- [49] W. Altmannshofer, C. Niehoff and D. M. Straub, *$B_s \rightarrow \mu^+\mu^-$ as current and future probe of new physics*, *JHEP* **05** (2017) 076, [[1702.05498](#)].
- [50] C.-H. Chen, T. Nomura and H. Okada, *Excesses of muon $g-2$, $R_{D^{(*)}}$, and R_K in a leptoquark model*, [[1703.03251](#)].
- [51] A. Greljo, G. Isidori and D. Marzocca, *On the breaking of Lepton Flavor Universality in B decays*, *JHEP* **07** (2015) 142, [[1506.01705](#)].
- [52] A. K. Alok, D. Kumar, S. Kumbhakar and S. U. Sankar, *D^* polarization as a probe to discriminate new physics in $B \rightarrow D^* \tau \nu$* , [[1606.03164](#)].
- [53] M. A. Ivanov, J. G. Krner and C.-T. Tran, *Analyzing new physics in the decays $\bar{B}^0 \rightarrow D^{(*)}\tau^-\bar{\nu}_\tau$ with form factors obtained from the covariant quark model*, *Phys. Rev.* **D94** (2016) 094028, [[1607.02932](#)].
- [54] D. A. Faroughy, A. Greljo and J. F. Kamenik, *Confronting lepton flavor universality violation in B decays with high- p_T tau lepton searches at LHC*, *Phys. Lett.* **B764** (2017) 126–134, [[1609.07138](#)].
- [55] F. Feruglio, P. Paradisi and A. Pattori, *Revisiting Lepton Flavor Universality in B Decays*, *Phys. Rev. Lett.* **118** (2017) 011801, [[1606.00524](#)].
- [56] P. Biancofiore, P. Colangelo and F. De Fazio, *Rare semileptonic $B \rightarrow K^*\ell^+\ell^-$ decays in RS_c model*, *Phys. Rev.* **D89** (2014) 095018, [[1403.2944](#)].
- [57] P. Biancofiore, P. Colangelo, F. De Fazio and E. Scrimieri, *Exclusive $b \rightarrow s\nu\bar{\nu}$ induced transitions in RS_c model*, *Eur. Phys. J.* **C75** (2015) 134, [[1408.5614](#)].
- [58] A. Carmona and F. Goertz, *Lepton Flavor and Nonuniversality from Minimal Composite Higgs Setups*, *Phys. Rev. Lett.* **116** (2016) 251801, [[1510.07658](#)].
- [59] I. García García, *LHCb anomalies from a natural perspective*, *JHEP* **03** (2017) 040, [[1611.03507](#)].
- [60] C. Bobeth, G. Hiller and G. Piranishvili, *Angular distributions of $\bar{B} \rightarrow \bar{K}\ell^+\ell^-$ decays*, *JHEP* **12** (2007) 040, [[0709.4174](#)].
- [61] M. Bordone, G. Isidori and A. Pattori, *On the Standard Model predictions for R_K and R_{K^*}* , *Eur. Phys. J.* **C76** (2016) 440, [[1605.07633](#)].
- [62] D. Das, G. Hiller, M. Jung and A. Shires, *The $\bar{B} \rightarrow \bar{K}\pi\ell\ell$ and $\bar{B}_s \rightarrow \bar{K}K\ell\ell$ distributions at low hadronic recoil*, *JHEP* **09** (2014) 109, [[1406.6681](#)].

- [63] LHCb collaboration, R. Aaij et al., *Angular analysis of the $B^0 \rightarrow K^{*0} \mu^+ \mu^-$ decay using 3 fb^{-1} of integrated luminosity*, *JHEP* **02** (2016) 104, [[1512.04442](#)].
- [64] LHCb, CMS collaboration, V. Khachatryan et al., *Observation of the rare $B_s^0 \rightarrow \mu^+ \mu^-$ decay from the combined analysis of CMS and LHCb data*, *Nature* **522** (2015) 68–72, [[1411.4413](#)].
- [65] C. Bobeth, M. Gorbahn, T. Hermann, M. Misiak, E. Stamou and M. Steinhauser, *$B_{s,d} \rightarrow l^+ l^-$ in the Standard Model with Reduced Theoretical Uncertainty*, *Phys. Rev. Lett.* **112** (2014) 101801, [[1311.0903](#)].
- [66] T. Hurth, F. Mahmoudi and S. Neshatpour, *On the anomalies in the latest LHCb data*, *Nucl. Phys.* **B909** (2016) 737–777, [[1603.00865](#)].
- [67] F. Mahmoudi, T. Hurth and S. Neshatpour, *Present Status of $b \rightarrow s \ell^+ \ell^-$ Anomalies*, *Nucl. Part. Phys. Proc.* **285-286** (2017) 39–44, [[1611.05060](#)].
- [68] B. Capdevila, S. Descotes-Genon, J. Matias and J. Virto, *Assessing lepton-flavour non-universality from $B \rightarrow K^* \ell \ell$ angular analyses*, *JHEP* **10** (2016) 075, [[1605.03156](#)].
- [69] B. Capdevila, S. Descotes-Genon, L. Hofer, J. Matias and J. Virto, *$B \rightarrow K^*(\rightarrow K \pi) \ell^+ \ell^-$ theory and the global picture: What’s next?*, *PoS LHCP2016* (2016) 073, [[1609.01355](#)].
- [70] W. Altmannshofer, C. Niehoff, P. Stangl and D. M. Straub, *Status of the $B \rightarrow K^* \mu^+ \mu^-$ anomaly after Moriond 2017*, *Eur. Phys. J.* **C77** (2017) 377, [[1703.09189](#)].
- [71] SLD ELECTROWEAK GROUP, DELPHI, ALEPH, SLD, SLD HEAVY FLAVOUR GROUP, OPAL, LEP ELECTROWEAK WORKING GROUP, L3 collaboration, S. Schael et al., *Precision electroweak measurements on the Z resonance*, *Phys. Rept.* **427** (2006) 257–454, [[hep-ex/0509008](#)].
- [72] A. Falkowski, M. Gonzalez-Alonso and K. Mimouni, *Compilation of low-energy constraints on 4-fermion operators in the SMEFT*, [[1706.03783](#)].
- [73] ATLAS collaboration, M. Aaboud et al., *Search for high-mass new phenomena in the dilepton final state using proton-proton collisions at $\sqrt{s} = 13 \text{ TeV}$ with the ATLAS detector*, *Phys. Lett.* **B761** (2016) 372–392, [[1607.03669](#)].
- [74] CMS collaboration, V. Khachatryan et al., *Search for heavy resonances decaying to tau lepton pairs in proton-proton collisions at $\sqrt{s} = 13 \text{ TeV}$* , *JHEP* **02** (2017) 048, [[1611.06594](#)].
- [75] ATLAS collaboration, G. Aad et al., *A search for $t\bar{t}$ resonances using lepton-plus-jets events in proton-proton collisions at $\sqrt{s} = 8 \text{ TeV}$ with the ATLAS detector*, *JHEP* **08** (2015) 148, [[1505.07018](#)].
- [76] B. Lillie, L. Randall and L.-T. Wang, *The Bulk RS KK-gluon at the LHC*, *JHEP* **09** (2007) 074, [[hep-ph/0701166](#)].

- [77] CMS collaboration, S. Chatrchyan et al., *Searches for new physics using the $t\bar{t}$ invariant mass distribution in pp collisions at $\sqrt{s}=8\text{TeV}$* , *Phys. Rev. Lett.* **111** (2013) 211804, [[1309.2030](#)].
- [78] K. Agashe, A. Belyaev, T. Krupovnickas, G. Perez and J. Virzi, *LHC Signals from Warped Extra Dimensions*, *Phys. Rev.* **D77** (2008) 015003, [[hep-ph/0612015](#)].
- [79] A. Greljo and D. Marzocca, *High- p_T dilepton tails and flavour physics*, [1704.09015](#).
- [80] G. Isidori, *Flavour Physics and Implication for New Phenomena*, *Adv. Ser. Direct. High Energy Phys.* **26** (2016) 339–355, [[1507.00867](#)].
- [81] BABAR collaboration, J. P. Lees et al., *Search for $B \rightarrow K^{(*)}\nu\bar{\nu}$ and invisible quarkonium decays*, *Phys. Rev.* **D87** (2013) 112005, [[1303.7465](#)].
- [82] BABAR collaboration, J. P. Lees et al., *Search for $B^+ \rightarrow K^+\tau^+\tau^-$ at the BaBar experiment*, *Phys. Rev. Lett.* **118** (2017) 031802, [[1605.09637](#)].
- [83] HPQCD collaboration, C. Bouchard, G. P. Lepage, C. Monahan, H. Na and J. Shigemitsu, *Standard Model Predictions for $B \rightarrow K\ell^+\ell^-$ with Form Factors from Lattice QCD*, *Phys. Rev. Lett.* **111** (2013) 162002, [[1306.0434](#)].
- [84] Y. Amhis et al., *Averages of b -hadron, c -hadron, and τ -lepton properties as of summer 2016*, [1612.07233](#).
- [85] F. U. Bernlochner, Z. Ligeti, M. Papucci and D. J. Robinson, *Combined analysis of semileptonic B decays to D and D^* : $R(D^{(*)})$, $|V_{cb}|$, and new physics*, *Phys. Rev.* **D95** (2017) 115008, [[1703.05330](#)].
- [86] A. Pich, *Precision Tau Physics*, *Prog. Part. Nucl. Phys.* **75** (2014) 41–85, [[1310.7922](#)].
- [87] E. Megias, M. Quiros and L. Salas, *$g_\mu - 2$ from Vector-Like Leptons in Warped Space*, *JHEP* **05** (2017) 016, [[1701.05072](#)].